INFORMATION TO USERS

This manuscript has been reproduced from the microfilm master. UMI films the text directly from the original or copy submitted. Thus, some thesis and dissertation copies are in typewriter face, while others may be from any type of computer printer.

The quality of this reproduction is dependent upon the quality of the copy submitted. Broken or indistinct print, colored or poor quality illustrations and photographs, print bleedthrough, substandard margins, and improper alignment can adversely affect reproduction.

In the unlikely event that the author did not send UMI a complete manuscript and there are missing pages, these will be noted. Also, if unauthorized copyright material had to be removed, a note will indicate the deletion.

Oversize materials (e.g., maps, drawings, charts) are reproduced by sectioning the original, beginning at the upper left-hand corner and continuing from left to right in equal sections with small overlaps. Each original is also photographed in one exposure and is included in reduced form at the back of the book.

Photographs included in the original manuscript have been reproduced xerographically in this copy. Higher quality 6" x 9" black and white photographic prints are available for any photographs or illustrations appearing in this copy for an additional charge. Contact UMI directly to order.

UMI

A Bell & Howell Information Company
300 North Zeeb Road, Ann Arbor MI 48106-1346 USA
313/761-4700 800/521-0600

An Analysis of Interferometric Measurements Using Quantum Phase Formalism

by

Brian Han

A dissertation submitted to the Graduate Faculty in Physics in partial fulfillment of the requirements for the degree of Doctor of Philosophy. The City University of New York

1999

This manuscript has been read and accepted for the Graduate Faculty in Physics in satisfaction of the dissertation requirement for the degree of Doctor of Philosophy.

1/25/99
Date

Mark Hillery
Professor Mark S. Hillery
Chair of Examining Committee

1/25/99
Date

Professor Louis S. Celenza
Executive Officer

Professor Janos Bergou

Professor Ying-Chin Chen

Professor Marten denBoer

Professor Alexander Lisyansky

Supervisory Committee

THE CITY UNIVERSITY OF NEW YORK

Abstract

An Analysis of Interferometric Measurements

Using the Quantum Phase Formalism

by

Brian Han

Advisor : Mark Hillery

Employing the quantum phase formalism. we investigate the sensitivity of an interferometer. This sensitivity depends on the state of light which enters the interferometer through the difference phase distribution of the state of the light it provides inside the interferometer. It is known from a semiclassical analysis that difference phase squeezing inside the interferometer can be achieved from amplitude squeezing of the input beams. Following this analysis. we study the effect of quantum amplitude squeezing of the input beams on the sensitivity using a squeezed state. We find that quantum amplitude squeezing enhances the accuracy of the interferometer.

We then study number state inputs with equal intensities which lead to light inside the interferometer with narrow peaks in the difference phase distribution.

We find that even though the peaks are narrow for this input state, effect of two peak structure inside the interferometer causes the signal to cancel. We also study the case for $|n,0\rangle$, input state with n number of photons and a vacuum state. We find that for $|n,0\rangle$ state the peak in the differnce phase distribuiton is located at $\frac{\pi}{2}$ with the width of the peak to be in the order of $\frac{1}{\sqrt{n}}$. Then we study the effect on the difference phase distribution of increasing photon numbers in one of the input ports from the zero, i.e. input states $|n,1\rangle$, $|n,2\rangle$ and so on. We also study how the input state which is a linear combination of number states behaves inside the inteferometer and find that we obtain the sensitivity for this input state to be in the order of $1/n$.

Finally, we examine the role of losses. These cause the phase distribution to spread and thereby reduce the accuracy to which the phase shift can be determined. We determine relations between how great the losses are, how much the accuracy is degraded.

Dedication

To my family: my mother and father, my brother Hui Won, and my wife

Acknowlegements

First of all, I would like to express my deepest gratitude to my thesis advisor and mentor, Professor Mark Hillery, for originally suggesting this study and for his invaluable help, patient guidance, and encouragement throughout the work. Under his influence, I have benefited greatly from his knowledge and insight.

A special note of thanks goes to Professor Janos Bergou for his invaluable suggestions in the early stages of this study, for his concern and help on this work thereafter, and for the excellent lectures and seminars he gave me in this field.

My thanks also go to Professor Ying-Chin Chen, Professor Marten denBoer, and Professor Alexander Lisyansky for their guidance and help as members of my thesis committee.

Finally, I really wish to thank my family for their unfailing support and encouragement. They always have been my sources of inspiration. Without their love, patience and sacrifice, I could have not come this far. For their total dedication to me, I am greatly indebted.

Table of contents

List of Figures

Chapter I

1 The measurement of phase inside an interferometer

1.1 Introduction

The modern quantum phase formalism was invented by Susskind and Glogower [1] in 1964. and expanded upon by Carruthers and Nieto in 1968 [2]. More recently, a series of papers by Pegg and Barnett stimulated considerable work in this area which both expanded the formalism and led to its application [4.5].

Here we would like to discuss the application of the quantum phase formalism to the analysis of the sensitivity of an interferometer. An interferometer has two input ports and two output ports. Light is sent into the two input ports. travels through the interferometer along two different paths. and emerges from the output ports where it is detected. In one of the paths in the interferometer. a phase shift is introduced, and by measuring the ouput light. this phase shift can be determined. The accuracy to which it can be measured depends on the state of light which enters the interferometer. If the input state consists of coherent states, the accuracy is $1/\sqrt{N}$, where N is the total number of photons in the

input state. With other kinds of light, an accuracy of $1/N$ can be achieved [6.7].

The place in the interferometer where employing the quantum phase formalism is useful is between the input and output ports. There one has a two-mode light state (one mode for each path), and the effect of a phase shift , ϕ, is to shift the phase difference distribution of this state by ϕ. One wants the phase shift to cause as large a change as possible in the state. The accuracy with which the phase shift can be measured is directly related to how distinguishable the two states before, $|\psi_a\rangle$, and after, $|\psi_b\rangle$, the phase shift, are. If the two states are almost orthogonal, then they are distinguishable and it is easy to tell whether the phase shift occurred or not. On the other hand, if the overlap between the states is large, then it is difficult to distinguish between them, and consequently, difficult to tell if a phase shift occurred . It can be shown that if the overlap between the phase distribution of two states is small, then the overlap between the states themselves is also small [8]. If the difference-phase distribution of $|\psi_a\rangle$ consists of a single narrow peak, then the difference-phase distribution of $|\psi_b\rangle$ also consists of a single peak, but the location of the peak is shifted by ϕ. If ϕ is larger than the width of the peak, then $|\psi_a\rangle$ and $|\psi_b\rangle$ are almost othogonal, and the existence of a phase shift can be easily inferred. Therefore, we can detect phase shifts larger than or comparable to the width of the peak, which implies that in order to detect small phase shifts, we want states $|\psi_a\rangle$ whose difference-phase distributions have narrow peaks.

A semiclassical analysis shows that for input fields of equal intensity, the initial beam splitter in a Mach-Zender interferometer converts intensity fluctuations into phase-difference fluctuations [9, 10]. This suggests that if the input state has squeezed intensity fluctuations, then the state after the beam splitter, which corresponds to the state $|\psi_a\rangle$, will have reduced phase difference fluctuations, i.e. exactly what we wish to achieve.

We begin this study with a more thorough analysis of the relation between the amplitude fluctuations at the input of a beam splitter and the phase difference fluctuations at its output. We examine the case of an input state consisting of two quadrature-squeezed states, and find that initially the squeezing improves the sensitivity, but if the squeezing becomes too great, then the sensitivity deteriorates. We also look at the case of an input state consisting of two number states with equal numbers of photons (for which the amplitude fluctuations are zero). This has been considered before [9, 10], and it has been shown that the difference-phase distribution of the state after the beam splitter has two peaks, one at 0 and at π [10]. We discuss why this two-peaked structure makes the usual method of measuring the photon-number difference at the output of interferometer to detect a phase shift useless, and examine a proposal to overcome this problem. We also consider the situation when the photon numbers entering the two input ports are not equal.

We finish by examining the role of losses. These cause phase distributions to

spread and thereby reduce the accuracy to which the phase shift can be determined. We determine relations between how great the losses are, and how much the accuracy is degraded.

1.2 Quantum phase formalism

In the classical theory of light waves, it is convenient to write the complex amplitude as a product of a real amplitude and a phase factor. We write the classical vector potential as $A_k = A_0 e^{i\phi}$ and for a single mode we can write it as

$$A = A_0\{\exp(-i\omega t + i\mathbf{k}\cdot\mathbf{r} + i\phi) + \exp(i\omega t - i\mathbf{k}\cdot\mathbf{r} - i\phi)\} \qquad (1.2.1)$$

It is similarly convenient in quantum mechanics to make a separation into amplitude and phase factors, analogous to equation (1.2.1). To do this, it is necessary to introduce the concept of phase into the quantum-mechanical description of the field. The single mode quantum mechanical vector potential operator is

$$A = (\hbar/2\epsilon_o V\omega)^{\frac{1}{2}}\{a\exp(-i\omega t + i\mathbf{k}\cdot\mathbf{r} + i\phi) + a^\dagger \exp(i\omega t - i\mathbf{k}\cdot\mathbf{r} - i\phi)\}. \quad (1.2.2)$$

The analog of equation (1.2.1) is thus a separation of a into a product of amplitude and phase operators. There is, in fact, no exact prescription for the way in which the separation should be accomplished in quantum mechanics and therefore, there is corresponding degree of arbitrariness in the defintion of the quantum mechanical phase operator. The main considerations are that the quantum mechanical

phase should have the same significance as the classical phase in the appropriate limit, and the phase should be associated with the Hermitian operators so that it is an observable quantity. [20]

According to Susskind and Glogower(SG) [1], and later Carruthers and Nieto [2], a is decompoesd as $(n+1)^{\frac{1}{2}}\exp(i\phi)$ and $a^\dagger$ as $\exp(-i\phi)(n+1)^{\frac{1}{2}}$ where the $\exp(i\phi)$ is defined as the exponetial phase operator and we have the following expressions for SG the phase operator

$$\exp(i\phi) = (n+1)^{-\frac{1}{2}}a \tag{1.2.3}$$

$$\exp(-i\phi) = a^\dagger(n+1)^{-\frac{1}{2}}. \tag{1.2.4}$$

Applying the phase operators to the number state, we have

$$\begin{aligned}\exp(i\phi)|n\rangle &= |n-1\rangle \quad \text{for } n \neq 0 \\ &= 0 \qquad\quad \text{for } n = 0\end{aligned} \tag{1.2.5}$$

$$\exp(-i\phi)|n\rangle = |n+1\rangle. \tag{1.2.6}$$

If we expand operator $\exp(i\phi)$ and $\exp(-i\phi)$ in the number state basis, we have

$$\exp(i\phi) = \sum_{n=0}^{\infty}|n\rangle\langle n+1| \tag{1.2.7}$$

$$\exp(-i\phi) = \sum_{n=0}^{\infty}|n+1\rangle\langle n|. \tag{1.2.8}$$

Thus, these two exponetial phase operators have non-vanishing matrix elements in the number state representation. These matrix elements are similar to those of the creation and destruction operators except they do not have the normalization

factors, $\sqrt{n}$ for a and $\sqrt{n+1}$ for $a^\dagger$. The "eigenstates" (these states cannot be normalized) for the SG phase operator are given by

$$|\phi\rangle = \sum_{n=0}^{\infty} e^{-in\phi}|n\rangle. \tag{1.2.9}$$

These operators are well defined but they are not unitary : since we have

$$aa^\dagger = n + 1 \tag{1.2.10}$$

it follows from equations (1.2.7) and (1.2.8) that

$$\exp(i\phi)\exp(-i\phi) = 1. \tag{1.2.11}$$

However, the reverse order product of the exponential operators is not equal to unity:

$$\exp(-i\phi)\exp(i\phi) = 1 - |0\rangle\langle 0|. \tag{1.2.12}$$

This can be expressed in the commutation relation

$$[e^{i\phi}, e^{-i\phi}] = |0\rangle\langle 0|. \tag{1.2.13}$$

The termination of the eigenvalue spectrum of n at zero is responsible for the non-unitarity of $e^{i\phi}$ and therefore, the non-existence of a conjugate Hermitian phase varibles, $\varphi = -i\log e^{i\phi}$. If we try to define commutation rules for the intensity and the phase analogous to those of position and momentum, then we end up having the eigenstates of the phase as $|\phi\rangle = \sum_{n=-\infty}^{\infty} e^{in\phi}|n\rangle$, and this violates the physical priciples; we can not have negative photon numbers.

The commutator

$$[x, p] = i \tag{1.2.14}$$

is satisfied if we let p act as a differential operator in the position space

$$p = -i\hbar(d/dx). \tag{1.2.15}$$

The momentum eigenfuctions are then $\langle x|p\rangle = \frac{1}{\sqrt{2\pi\hbar}} e^{\frac{i}{\hbar}xp}$. The position eigenkets is expanded in terms of momentum eigenkets which spans the same space

$$|x\rangle = \int dp|p\rangle\langle p|x\rangle \tag{1.2.16}$$

$$|p\rangle = \int dx|x\rangle\langle p|x\rangle. \tag{1.2.17}$$

If we try to use the analogy for n and ϕ,

$$[n, \phi] = i \tag{1.2.18}$$

$$n = i\frac{d}{d\phi} \tag{1.2.19}$$

then we have the eigenfunctions of n whose eigenvalues run from $-\infty$ to ∞ and therefore we would have phase state as [2]

$$|\phi\rangle = \sum_{n=-\infty}^{\infty} e^{-in\phi}|n\rangle. \tag{1.2.20}$$

Neverthless we note that the these state as defined in the equation (1.2.9) do provide a resolution of identity

$$\int_{\pi}^{\pi} d\phi|\phi\rangle\langle\phi| = 2\pi \tag{1.2.21}$$

and, for the phase distribution defined below for any state $|\psi\rangle$, there are theoretical grounds [11,12] for believing that it is the correct distribution for the optimal phase measurments.

$$P(\phi) = \frac{1}{2\pi}|\langle\phi|\psi\rangle|^2. \tag{1.2.22}$$

One can construct the Hermitian operators from the exponetial phase operators [2]

$$\cos(\phi) = \frac{1}{2}\{\exp(i\phi) + \exp(-i\phi)\} \tag{1.2.23}$$

$$\sin(\phi) = \frac{-i}{2}\{\exp(i\phi) - \exp -(i\phi)\}. \tag{1.2.24}$$

The eigenfunctions and eigenvalues for those Hermitian operators are

$$\cos\phi|\cos\phi\rangle = \cos\phi|\cos\phi\rangle \tag{1.2.25}$$

$$|\cos\phi\rangle = (\frac{1}{\pi})^{\frac{1}{2}}\sum_{n=0}^{\infty}\sin(n+1)\phi|n\rangle \tag{1.2.26}$$

$$\sin\phi|\sin\phi\rangle = \sin\phi|\sin\phi\rangle \tag{1.2.27}$$

$$|\sin\phi\rangle = (\frac{1}{\pi})^{\frac{1}{2}}\sum_{n=0}^{\infty}\{e^{(i(n+1)\phi)} - e^{(-i(n+1)(\phi-\pi))}\}|n\rangle. \tag{1.2.28}$$

1.3 Beam splitter

The beam splitter is a linear device and hence can be analyzed by considering the modes of a single frequency. The single mode fields will thus be sufficient for our present needs. In practice, beam spitter is a partially refecting mirror: some

of the incident light is transmitted and some reflected. (Fig. 1) Classically, it can be described in terms of a matrix,

$$\begin{pmatrix} E_1^{\text{out}} \\ E_2^{\text{out}} \end{pmatrix} = \begin{pmatrix} U_{11} & U_{12} \\ U_{21} & U_{22} \end{pmatrix} \begin{pmatrix} E_1^{\text{in}} \\ E_2^{\text{in}} \end{pmatrix} \tag{1.3.29}$$

where the actual field are

$$\vec{E}_j^{\text{in}}(\vec{r},t) = \hat{\epsilon}\,\text{Re}\,(\vec{E}_j^{\text{in}} e^{-i(\omega t - \vec{k}_j\cdot\vec{r})}) \tag{1.3.30}$$

and similarly we have

$$\vec{E}_j^{\text{out}}(\vec{r},t) = \hat{\epsilon}\,\text{Re}\,(\vec{E}_j^{\text{out}} e^{-i(\omega t - \vec{k}_j\cdot\vec{r})}). \tag{1.3.31}$$

The U_{ij} are complex numbers whose values depend on the detailed construction of the beam splitters. General physical consideration place some restrictions on the U_{ij}, however.

Quantum mechanically, using the correspondence between E_j^{in} and a_j, we have

$$\vec{E}_j^{(\text{in})(-)}(\vec{r},t) = -i\hat{\epsilon}\sqrt{\frac{\hbar\omega}{2\varepsilon_o}}\, a_j\, e^{-i(\omega t - \vec{k}_j\cdot\vec{r})} \tag{1.3.32}$$

where a_j is the annihilation operator in the input mode j and j runs 1 and 2. Similarly, we have

$$\vec{E}_j^{(\text{out})(-)}(\vec{r},t) = +i\hat{\epsilon}\sqrt{\frac{\hbar\omega}{2\varepsilon_o}}\, b_j\, e^{-i(\omega t - \vec{k}_j\cdot\vec{r})} \tag{1.3.33}$$

where b_j are the annihilation operators in the output mode j and j runs 1 and 2. In Fig. (1) we represented the annihilation operators in the output mode as

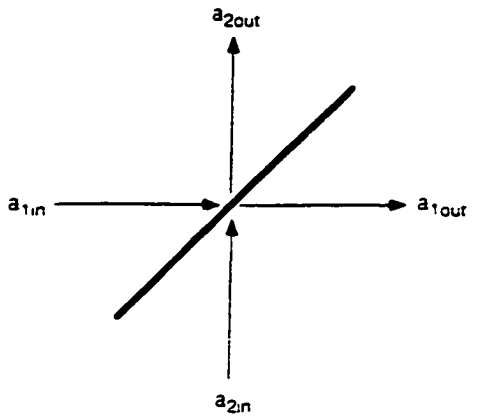

Figure 1: A beam splitter. The annihilation operator $a_{1\text{in}}$ and $a_{2\text{in}}$ correspond the input fields E_1^{in} and E_2^{in} respectively and $a_{1\text{out}}$ and $a_{2\text{out}}$ correspond the output fields E_1^{out} and E_2^{out} respectively. The output fields are related to the input fields via a unitary transformation.

$a_{j\text{out}}$. $b_j = a_{j\text{out}}$. Substituting (1.3.32) and (1.3.33) into (1.3.29), one obtains

$$\begin{pmatrix} b_1 \\ b_2 \end{pmatrix} = \begin{pmatrix} U_{11} & U_{12} \\ U_{21} & U_{22} \end{pmatrix} \begin{pmatrix} a_1 \\ a_2 \end{pmatrix}. \tag{1.3.34}$$

The beam splitter thus effectively performs a linear transformation on the annihilation operators. Before the incoming fields arrive at the beam splitters, they consist of two independent modes and hence must satisfy the commutation relations for the harmonic oscillator, i.e.,

$$[a_i, a_j] = 0 \tag{1.3.35}$$

$$[a_i, a_j^\dagger] = \delta_{ij} \tag{1.3.36}$$

for $i \in \{1,2\}$ and $j \in \{1,2\}$. Similarly, once the field has left the beam splitter, it propoagates as two separate modes which also satisfy commutation relations

$$[b_i , b_j] = 0 \tag{1.3.37}$$

$$[b_i , b_j^\dagger] = \delta_{i,j}. \tag{1.3.38}$$

Enforcing the above contraints leads to the following restrictions on the $U_{i,j}$:

$$\begin{aligned} |U_{11}|^2 + |U_{12}|^2 &= 1 \\ |U_{21}|^2 + |U_{22}|^2 &= 1 \\ U_{11}U_{21}^* + U_{12}U_{22}^* &= 0. \end{aligned} \tag{1.3.39}$$

This is equivalent to saying that the matrix

$$U = \begin{pmatrix} U_{11} & U_{12} \\ U_{21} & U_{22} \end{pmatrix} \tag{1.3.40}$$

is unitary, i.e.,

$$UU^\dagger = U^\dagger U = 1. \tag{1.3.41}$$

Hence the mode transformation performed by a beam splitter must be unitary if it is consistent with quantum mechanics. From the equations (1.3.39), we have

$$|U_{11}|^2 = |U_{22}|^2 = T \tag{1.3.42}$$

and

$$|U_{12}|^2 = |U_{21}|^2 = R \tag{1.3.43}$$

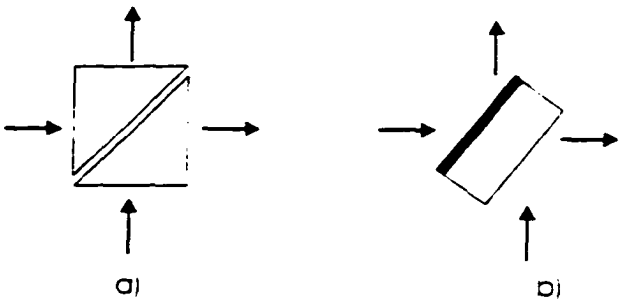

Figure 2: An example of a symmetric beam splitter and an asymmetric beam splitter. a) The symmetric beam splitter consists of two back-to-back prisms with an air gap in between. b) The asymmetric beam splitter consists of a plate of glass that has been partly silvered on one side.

where T and R denote respectively the transmission and reflection coefficients. In principle, any unitary transformation (1.3.39) can be realized by suitably engineering the beam splitter. For example, the symmetric unitary transformation

$$U = \begin{pmatrix} \sqrt{T} & i\sqrt{R} \\ i\sqrt{R} & \sqrt{T} \end{pmatrix} \tag{1.3.44}$$

might be realized by a symmetric beam splitter constructed by two back-to-back prisms with an air gap between. (Fig. 2) An antisymmetric beam splitter

$$U = \begin{pmatrix} \sqrt{T} & \sqrt{R} \\ -\sqrt{R} & \sqrt{T} \end{pmatrix} \tag{1.3.45}$$

might be constructed by, for example, silvering a glass plate on one side. (Fig.

2)

Classical analysis shows that if a stream of n photons is incident on the beam splitter, then the probability that the k photons are transmitted and $n-k$ photons are reflected is

$$P(k, n-k) = \frac{n!}{k!(n-k)!} T^k R^{n-k}. \tag{1.3.46}$$

Quantum mechanically, the beam splitter performs the unitary transformation

$$b_1 = U_{11} a_1 + U_{12} a_2$$

$$b_2 = U_{21} a_1 + U_{22} a_2 \tag{1.3.47}$$

where a_1 and a_2 are the two input modes and b_1 and b_2 are the two output modes. Inverting equation (1.3.47), we have

$$a_1 = U_{11}^* b_1 + U_{21}^* b_2$$

$$a_2 = U_{12}^* b_1 + U_{22}^* b_2. \tag{1.3.48}$$

The system we wish to consider is one which n photons are entering the a_1 port of the beam splitter

$$|\psi\rangle = \frac{[a_1^\dagger]^n}{\sqrt{n!}} |0\rangle. \tag{1.3.49}$$

From (1.3.48), we have

$$[a_1]^n = \sum_{k=0}^{n} \frac{n!}{k!(n-k)!} [U_{11}]^k [U_{21}]^{n-k} [b_1^\dagger]^k [b_2^\dagger]^{k-n}. \tag{1.3.50}$$

Therefore, in terms of the number basis $|m, n; \text{out}\rangle$

$$|m, n; \text{out}\rangle = \frac{[b_1^\dagger]^m}{\sqrt{m!}} \frac{[b_2^\dagger]^n}{\sqrt{n!}} |0, 0\rangle \tag{1.3.51}$$

one has

$$|\psi\rangle = \sum_{k=0}^{n} \left(\frac{n!}{k!(n-k)!}\right)^{\frac{1}{2}} [U_{11}]^k [U_{21}]^{n-k} |k, n-k; \text{out}\rangle. \tag{1.3.52}$$

The probability amplitude that k photons are transmitted is thus

$$\langle k, n-k; \text{out}|\psi\rangle = \left(\frac{n!}{k!(n-k)!}\right)^{\frac{1}{2}} U_{11}^k U_{21}^{n-k} \tag{1.3.53}$$

The probability $P(k, n-k)$ is just the norm squared of this amplitude

$$P(k, n-k) = |\langle k, n-k; \text{out}|\psi\rangle|^2 \tag{1.3.54}$$

and therefore,we have

$$P(k, n-k) = \frac{n!}{k!(n-k)!} T^k R^{n-k} \tag{1.3.55}$$

where the transmission and reflectin coefficients are given by

$$T = |U_{11}|^2$$

$$R = |U_{21}|^2. \tag{1.3.56}$$

Equation (1.3.46) is identical to equation (1.3.55). Therefore, when light enters only one port of a beam splitter, the photons are partioned randomly as if they were statistically independent particles; photons display classical-like particle behavior if the photons enters only one input port of a beam splitter. However, photons have also wavelike properties. If two light beams enter a beam spitter, they will interfere with each other. For a 50-50 beam splitter, one finds that if two identical one-photon wave packets enter the beam splitter, both will exit

through the same port. Let's we consider case where a single photon enters each input port

$$|\psi\rangle = a_1^\dagger a_2^\dagger . |0\rangle \tag{1.3.57}$$

Using the inverse transformation equation (1.3.48), one obtains

$$\begin{aligned} |\psi\rangle &= 2^{\frac{1}{2}} U_{11} U_{12} |2.0; \text{out}\rangle \\ &+ 2^{\frac{1}{2}} U_{21} U_{22} |0.2; \text{out}\rangle \\ &+ [U_{11} U_{22} + U_{12} U_{21}] \| 1.1; \text{out}\rangle \end{aligned} \tag{1.3.58}$$

where

$$|2.0; \text{out}\rangle = \frac{[b_1^\dagger]^2}{\sqrt{2}} |0\rangle \tag{1.3.59}$$

is the state in which both photons exit through port # 1.

$$|0.2; \text{out}\rangle = \frac{[b_2^\dagger]^2}{\sqrt{1}} |0\rangle \tag{1.3.60}$$

is the state for which both photons exit through port #2. and

$$|1.1; \text{out}\rangle = b_1^\dagger b_2^\dagger |0\rangle \tag{1.3.61}$$

is the state for which each photon exits a different port. The U_{ij} can be expressed in the followng form

$$\begin{aligned} U_{11} &= T^{1/2} e^{i\varphi_{11}} \\ U_{12} &= R^{1/2} e^{i\varphi_{12}} \\ U_{21} &= R^{1/2} e^{i\varphi_{21}} \\ U_{22} &= T^{1/2} e^{i\varphi_{22}} \end{aligned} \tag{1.3.62}$$

where T and R are the transmission and reflection coefficients respectively. Since unitarity requires that the U_{ij} satisfy

$$U_{11}U_{21}^{*} + U_{12}U_{22}^{*} = 0. \tag{1.3.63}$$

the ϕ_{ij} are not independent but must satisfy

$$e^{i(\phi_{11}+\phi_{22})} = -e^{i(\phi_{12}+\phi_{21})}. \tag{1.3.64}$$

Equation (1.3.58) can thus be put into the form

$$\begin{aligned} |\psi\rangle = \sqrt{2TR}[&e^{i(\phi_{11}+\phi_{12})}|2,0;\text{out}\rangle \\ &+e^{i(\phi_{21}+\phi_{22})}|0,2;\text{out}\rangle] \\ &+(T-R)e^{i(\phi_{11}+\phi_{22})}|1,1;\text{out}\rangle. \end{aligned} \tag{1.3.65}$$

The minus sign in the third term of the equation (1.3.58) can be interpreted as destructive interference between the probability amplitude for the process in which both particles are transmitted through the beam splitter and the probability amplitude that both particles are reflected from the beam splitter. When $T = R$, that is , when one has 50-50 beam splitter, the destructive interference is complete and one has

$$|\psi\rangle = \sqrt{2TR}[e^{i(\phi_{11}+\phi_{22})}|2,0;\text{out}\rangle + e^{i(\phi_{12}+\phi_{21})}]|0,2;\text{out}\rangle]. \tag{1.3.66}$$

Hence, both photons exit through the same port. These cases are illustrated in Fig. (3).

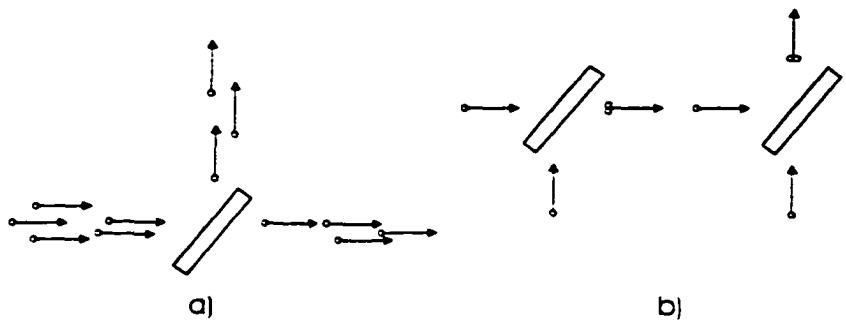

Figure 3: a) When photons enter only one input port of the beam splitter, the photons are partitioned randomly between the two output ports. b) Because of photon interference effect when two identical photons enter a beam splitter, one in each port, both photons must exit through the same output port.

The above discussion can be generalized to the case when n photons enter each of the two input ports of the beam splitter. The state vector in this case is

$$|\psi\rangle = \frac{[a_1^\dagger a_2^\dagger]^n}{n!}|0\rangle. \tag{1.3.67}$$

Now for the 50-50 beam splitter

$$a_1^\dagger a_2^\dagger = \frac{1}{2}[e^{i(\phi_{11}+\phi_{12})}b_1^\dagger b_1^\dagger + e^{-i(\phi_{21}+\phi_{22})}b_2^\dagger b_2^\dagger]. \tag{1.3.68}$$

so

$$[a_1^\dagger a_2^\dagger]^n = \frac{1}{2^n}\sum_{k=0}^{n}\frac{n!}{k!(n-k)!}e^{ik(\phi_{11}+\phi_{12})}e^{i(n-k)(\phi_{21}+\phi_{22})}(b_1^\dagger)^{(2k)}(b_2^\dagger)^{2(n-k)}. \tag{1.3.69}$$

Substituting this into Eq.(1.3.69), one finds

$$|\psi\rangle = \frac{1}{2^n n!}\sum_{k=0}^{n}\frac{n!}{k!(n-k)!}\{\ [(2k)!(2n-2k)!]^{1/2}$$

$$e^{ik(\phi_{11}+\phi_{12})}e^{i(n-k)(\phi_{21}+\phi_{22})}|2k, 2(n-k); \text{out}\rangle \ \} \tag{1.3.70}$$

where

$$|2k, 2(n-k); out\rangle = \frac{[b_1^\dagger]^{2k}[b_2^\dagger]^{2(n-k)}}{\sqrt{(2k)!(2n-2k)!}}|0\rangle. \tag{1.3.71}$$

From Eq (1.3.71) one sees that the number of photons in either output beams is always even. This phenomenon can not be explained by treating the photons as non-interacting classical particles. Much of the discussion in this section is based on the work of Yurke. [21]

1.4 Coherent state input

The coherent state $|\alpha\rangle$ [13] is generated by applying the displacement operator $D(\alpha) = e^{(\alpha a^\dagger - \alpha^* a)}$ on the vacuum state

$$|\alpha\rangle = D(\alpha)|0\rangle. \tag{1.4.72}$$

Now, if we send the two coherent state $|\alpha_1\rangle$ and $|\alpha_2\rangle$ as our input beams to the beam splitter

$$|\psi; \text{in}\rangle = |\alpha_1, \alpha_2; \text{in}\rangle = (D(\alpha_1)_{\text{in}}D(\alpha_2)_{\text{in}})|0\rangle. \tag{1.4.73}$$

In order to see what comes out after the beam splitter for the coherent state input, we express in mode operators,a_j, in terms of the out mode operators, b_j.

using the equation (1.3.48)

$$\begin{pmatrix} a_1 \\ a_2 \end{pmatrix} = \begin{pmatrix} U_{11}^* & U_{21}^* \\ U_{12}^* & U_{22}^* \end{pmatrix} \begin{pmatrix} b_1 \\ b_2 \end{pmatrix}. \tag{1.4.74}$$

We can also have for the creation operators

$$\begin{pmatrix} a_1^\dagger \\ a_2^\dagger \end{pmatrix} = \begin{pmatrix} U_{11} & U_{21} \\ U_{12} & U_{22} \end{pmatrix} \begin{pmatrix} b_1^\dagger \\ b_2^\dagger \end{pmatrix}. \tag{1.4.75}$$

Expressing the displacement operator, $D(\alpha)$, in terms of out quantities, we have

$$\begin{aligned} (D(\alpha)_1)_{\text{in}} &= e^{\alpha_1 a_1^\dagger - \alpha_1^* a_1} \\ &= e^{\alpha_1(U_{11}b_1^\dagger + U_{21}b_2^\dagger) - \alpha_1^*(U_{11}^* b_1^\dagger + U_{21}^* b_2^\dagger)} \end{aligned} \tag{1.4.76}$$

and

$$\begin{aligned} (D(\alpha)_2)_{\text{in}} &= e^{\alpha_2 a_2^\dagger - \alpha_2^* a_2} \\ &= e^{\alpha_2(U_{12}b_1^\dagger + U_{22}b_2^\dagger) - \alpha_2^*(U_{12}^* b_1^\dagger + U_{22}^* b_2^\dagger)}. \end{aligned} \tag{1.4.77}$$

Therefore, we can now express the displacement operator in terms of out operators, b_1 and b_2. Rearranging the equation (1.4.73) in terms of out operators we have

$$|\psi_{\text{in}}\rangle = e^{(\alpha_1 U_{11} + \alpha_2 U_{12})b_1^\dagger - (\alpha_1^* U_{11}^* + \alpha_2^* U_{12}^*)b_1} e^{(\alpha_1 U_{21} + \alpha_2 U_{22})b_2^\dagger - (\alpha_1^* U_{21}^* + \alpha_2^* U_{22}^*)b_2} |0\rangle. \tag{1.4.78}$$

If we define,

$$\begin{pmatrix} \beta_1 \\ \beta_2 \end{pmatrix} = \begin{pmatrix} U_{11} & U_{12} \\ U_{21} & U_{22} \end{pmatrix} \begin{pmatrix} \alpha_1 \\ \alpha_2 \end{pmatrix} \tag{1.4.79}$$

then we have for the equation (1.4.78)

$$|\psi;\text{in}\rangle = |\beta_1, \beta_2\rangle = e^{\beta_1 b_1^\dagger - \beta_1^* b_1} e^{\beta_2 b_2^\dagger - \beta_2^* b_2}|0\rangle. \tag{1.4.80}$$

This is just two coherent states in the output modes. Quantum mechanically, the beam splitter transforms two coherent state inputs to two coherent state ouputs with the ouput amplitudes related to the input amplitudes classically

$$|\upsilon;\text{out}\rangle = U_{BS}|\upsilon;\text{in}\rangle \tag{1.4.81}$$

where U_{BS} represents the actions of the beam splitter on the incoming fields. In the Heisenberg picture, we have

$$\begin{pmatrix} b_1 \\ \\ b_2 \end{pmatrix} = U_{BS}^{-1} \begin{pmatrix} a_1 \\ \\ a_2 \end{pmatrix} U_{BS} \tag{1.4.82}$$

$$= \begin{pmatrix} U_{11} & U_{12} \\ \\ U_{21} & U_{22} \end{pmatrix} \begin{pmatrix} a_1 \\ \\ a_2 \end{pmatrix}. \tag{1.4.83}$$

1.5 Mach-Zender Interferometer

A Mach-Zender interferometer [14] consists of two beam splitters and a phase shifter. Each beam splitter has two input ports and two output ports as shown in Fig. 4. Using a group theoretical approach, Yurke, McCall, and Klauder elegantly showed [6] the connection between the group SU(2) and a beam splitter. Since SU(2) is equivalent to the rotation group, this will allow one to visualize the

operations of beam splitters and phase shifters as rotations in 3-space. Let's define the following operators [6]

$$\begin{aligned} J_1 &= (a_1^\dagger a_2 + a_1 \hat{a}_2^\dagger)/2. \\ J_2 &= -i(a_1^\dagger a_2 - a_1 a_2^\dagger)/2. \\ J_3 &= (a_1^\dagger a_1 - a_2 a_2^\dagger)/2. \end{aligned} \tag{1.5.84}$$

and

$$N = a_1^\dagger a_1 + a_2^\dagger a_2. \tag{1.5.85}$$

The operators in equation (1.5.84) are the Schwinger representation of the angular-momentum operators [15]. They obey the SU(2) commutation relations

$$[J_k, J_m] = i\epsilon_{kmn} J_n \tag{1.5.86}$$

where k, m and n run from 1 to 3 and ϵ_{kmn} is the completely antisymmetric tensor of rank 3. The Casimir invariant for this group can be put into the form

$$J^2 = \frac{N}{2}\left[(\frac{N}{2} + 1)\right] \tag{1.5.87}$$

The scattering matrix of a beam splitter, $U = \begin{pmatrix} U_{11} & U_{12} \\ U_{21} & U_{22} \end{pmatrix}$, will in general transform $(J_1\ J_2\ J_3)$ among themselves.

Consider a beam splitter with the scattering mattrix which is effectively equation (1.3.44) where we replace the $\sqrt{T}$ by $\cos(\frac{\alpha}{2})$ and $\sqrt{R}$ by $-\sin(\frac{\alpha}{2})$.

$$U = \begin{bmatrix} \cos(\frac{\alpha}{2}) & -i\sin(\frac{\alpha}{2}) \\ -i\sin(\frac{\alpha}{2}) & \cos(\frac{\alpha}{2}) \end{bmatrix} \tag{1.5.88}$$

This transformation will transform $\vec{J}$ according to

$$\begin{bmatrix} J_1 \\ J_2 \\ J_3 \end{bmatrix}_{\text{out}} = \begin{bmatrix} 1 & 0 & 0 \\ 0 & \cos(\alpha) & -\sin(\alpha) \\ 0 & \sin(\alpha) & \cos(\alpha) \end{bmatrix} \begin{bmatrix} J_1 \\ J_2 \\ J_3 \end{bmatrix}_{\text{in}} . \tag{1.5.89}$$

Thus the action of this beam spliitter is to rotate the abstract angular momentum vector, $\vec{J}$, about the x axis by an angle of α. This transformation can be expressed in the form

$$\begin{bmatrix} J_1 \\ J_2 \\ J_3 \end{bmatrix}_{\text{out}} = e^{i\alpha J_1} \begin{bmatrix} J_1 \\ J_2 \\ J_3 \end{bmatrix}_{\text{in}} e^{-i\alpha J_1} . \tag{1.5.90}$$

This equivalence of (1.5.89) and (1.5.90) can be checked using the operator identity

$$e^{\beta A} B e^{-\beta A} = B + \beta[A, B] + \frac{\beta^2}{2!}[A, [A, B]] + \ldots . \tag{1.5.91}$$

We can also work in a Schrödinger picture. Suppose that we have an input state $|\psi; \text{in}\rangle$ and we want to evaluate some observable, $F(a_{1\text{out}} a_{2\text{out}})$ at the output of a beam splitter, then we have

$$\begin{aligned} \langle \psi; \text{in}|F(a_{1\text{out}} a_{2\text{out}})|\psi; \text{in}\rangle &= \langle \psi; \text{in}|F(U_{\text{BS}}^{-1} a_{1\text{in}} U_{\text{in}}, U_{\text{BS}}^{-1} a_{2\text{in}} U_{\text{in}})|\psi; \text{in}\rangle \\ &= \langle \psi; \text{in}|U_{\text{BS}}^{-1} F(a_{1\text{in}} a_{2\text{in}}) U_{\text{BS}}|\psi; \text{in}\rangle . \end{aligned} \tag{1.5.92}$$

Therefore, if we define $|\psi; \text{out}\rangle = U_{\text{BS}}|\psi; \text{in}\rangle$, then we have

$$\langle \psi; \text{in}|F(a_{1\text{out}} a_{2\text{out}})|\psi; \text{in}\rangle = \langle \psi; \text{out}|F(a_{1\text{in}} a_{2\text{in}})|\psi; \text{out}\rangle . \tag{1.5.93}$$

In the Schrödinger picture the operators, J_1, J_2, J_3 do not change but the state vectors do.

As was shown by Yurke, McCall, and Klauder [6], a Mach-Zender interferometer can be described in terms of these operators alone. This is because what is measured at the ouput of the interferometer is J_3 and the beam-splitter transformations act like rotations which transform the angular momentum operators among themselves. Therefore, the measurement of J_3 at the output corresponds the measurements of a linear combination of J_1, J_2, and J_3 at the input.

The operator U can be expressed as the exponential of i times a linear combination of the operators in Eq. (1.5.84) [6.16]. We shall be interested in two particular examples. The first is described by the operator $U_1 = \exp(-i\pi J_1/2)$, which corresponds to the 2×2 matrix

$$\begin{bmatrix} a_{1\text{out}} \\ a_{2\text{out}} \end{bmatrix} = 1/\sqrt{2} \begin{bmatrix} 1 & -i \\ -i & 1 \end{bmatrix} \begin{bmatrix} a_{1\text{in}} \\ a_{2\text{in}} \end{bmatrix} \tag{1.5.94}$$

and the second is given by $U_2 = \exp(i\pi J_1/2)$, which corresponds to

$$\begin{bmatrix} a_{1\text{out}} \\ a_{2\text{out}} \end{bmatrix} = 1/\sqrt{2} \begin{bmatrix} 1 & i \\ i & 1 \end{bmatrix} \begin{bmatrix} a_{1\text{in}} \\ a_{2\text{in}} \end{bmatrix}. \tag{1.5.95}$$

We are now ready to form a Mach-Zender interferometer(see Fig. 4). The first beam splitter is described by U_1 and the second by U_2. The device producing a phase shift ϕ in one of the legs is described by the unitary operator $U(\phi)$= $\exp(-i\phi a_1^\dagger a_1)$. It produces the phase shift which we want to measure. After the

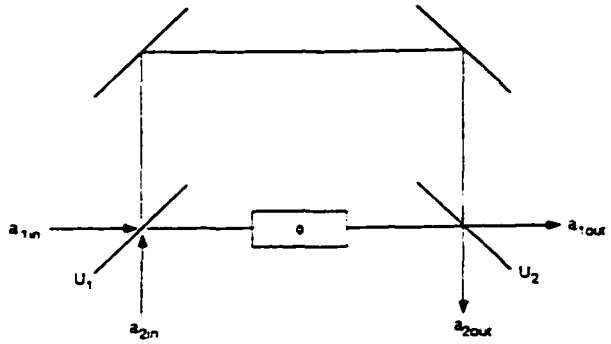

Figure 4: A Mach-Zehnder interferometer. The first beam splitter is described by the unitary operator U_1 and the second operator U_2. The device between the beam splitter, phase shiftor, produces a phase shift ϕ.

first beam splitter, the out operators b_1 and b_2 are related to in operators by the equation (1.5.94)

$$\begin{bmatrix} b_1 \\ b_2 \end{bmatrix} = 1/\sqrt{2} \begin{bmatrix} 1 & -i \\ -i & 1 \end{bmatrix} \begin{bmatrix} a_1 \\ a_2 \end{bmatrix}. \tag{1.5.96}$$

After the first beam splitter, the two beams propagate along different paths and one of the beam is going through the phase shifter. These changes in the operators are represented by

$$\begin{bmatrix} c_1 \\ c_2 \end{bmatrix} = \begin{bmatrix} e^{-i(\phi_1+\phi)} & 0 \\ 0 & e^{-i(\phi_2)} \end{bmatrix} \begin{bmatrix} b_1 \\ b_2 \end{bmatrix}. \tag{1.5.97}$$

For the second beam splitter, we have

$$\begin{bmatrix} d_1 \\ d_2 \end{bmatrix} = 1/\sqrt{2} \begin{bmatrix} 1 & i \\ i & 1 \end{bmatrix} \begin{bmatrix} c_1 \\ c_2 \end{bmatrix}. \tag{1.5.98}$$

Putting them all together and assuming $\phi_1 = \phi_2$, we have

$$\begin{bmatrix} d_1 \\ d_2 \end{bmatrix} = e^{-i(\phi_1+\frac{\varphi}{2})} \begin{bmatrix} \cos(\frac{\varphi}{2}) & -\sin(\frac{\varphi}{2}) \\ \sin(\frac{\varphi}{2}) & \cos(\frac{\varphi}{2}) \end{bmatrix} \begin{bmatrix} a_1 \\ a_2 \end{bmatrix}. \tag{1.5.99}$$

What we measure is the photon number differences at the outport which is $d_1^\dagger d_1 - d_2^\dagger d_2$. From equation (1.5.99), we have

$$d_1^\dagger d_1 - d_2^\dagger d_2 = \cos\varphi(a_1^\dagger a_1 - a_2^\dagger a_2) - \sin\varphi(a_1^\dagger a_2 - a_1 a_2^\dagger). \tag{1.5.100}$$

If we consider the interferometer as a whole, the output state is related to the input by

$$|\text{out}\rangle = U_2 U(\varphi) U_1 |\text{in}\rangle. \tag{1.5.101}$$

In order to measure changes in the phase shift φ, we usually meassure the difference between the photon numbers at the output ports, i.e.,

$$J_3 = (a_1^\dagger a_1 - a_2^\dagger a_2^\dagger)/2 \ . \tag{1.5.102}$$

Changes $\delta\varphi$ in the phase angle are detected by the changes they create in the expectation value of $J_{3\text{out}}$. Since there are fluctuations in $J_{3\text{out}}$, a phase change is detectable only if it induces a change in $\langle J_{3\text{out}}\rangle$ which is larger than than ΔJ_{3out}. Therefore, the minimum detectable phase change is given by

$$\delta\phi = \Delta J_{3\text{out}} / \left| \frac{d\langle J_{3\text{out}}\rangle}{d\varphi} \right|. \tag{1.5.103}$$

We are interested in which input states will produce a small value of $\delta\phi$. so it is useful to express equation (1.5.103) in terms of the input state. Using (1.5.89). one finds that

$$\begin{aligned} \langle J_{3\text{out}} \rangle &= \langle \text{out}|J_3|\text{out}\rangle \\ &= -\sin\phi\langle \text{in}|J_{1in}|\text{in}\rangle + \cos\phi\langle \text{in}|J_{3in}|\text{in}\rangle \end{aligned} \tag{1.5.104}$$

from which one concludes that

$$\frac{d\langle J_{3\text{out}}\rangle}{d\phi} = -\cos\phi\langle \text{in}|J_{1in}|\text{in}\rangle - \sin\phi\langle \text{in}|J_{3\text{in}}|\text{in}\rangle \tag{1.5.105}$$

To consider small changes about $\phi = 0$ we evaluate the equation (1.5.103). at $\phi = 0$. The quantity to be measured. usually a phase shift. is determined by measuring the difference in the number of photons emerging from the two output ports. The minimum shift which one can measure. the accuracy of the interferometer. is determined by the fluctuation in the input light. If a coherent state is sent into one of the input ports and the vacuum into the other. then the accuracy. $\delta\phi$. is $1/(|\alpha|) = 1/(\sqrt{N_{in}})$. where N_{in} is the mean number of photons in the input state. $N_{in} = \langle a^\dagger_{1in}a_{1in} + a^\dagger_{2in}a_{2in}\rangle$. If a standard squeezed state with squeezing parameter $r > 0$ is sent into the second port instead of the vacuum. then the accuracy becomes $e^{(-r)}/\sqrt{N}$. It is possible to do better. This was shown by Yurke. McCall. and Klauder [6]. They showed that a Mach-Zender interferometer can be analyzed using the group SU(2) and other interferometers. in which the beam splitters are replaced by four-wave mixers. can be analyzed using SU(1.1). These

observations have been employed by them and subsequent authors to examine how different input states are transformed by beam splitters and four-wave mixers [16,17]. Their group-theoretical analysis allowed Yurke, McCall, and Klauder to find an input state which allows one to measure a phase shift of order $1/N$. Also, Hillery and Mlodinow [8] achieved the same degree of minimum sensitivity, $\delta\phi = 1/N$, using the su(2) minimum uncertainty states.

Chapter II

2 The input state with reduced number fluctuation

2.1 Classical analysis

Hillery, Zou, and and Buzek [10] examined the phase properties of the beamsplitter output. It is the behaviour of the phase difference between the output beams which determines how the beamsplitter will behave as part of an interferometer. They studied a beam splitter which relates two classical input fields to two classical output fields as

$$\begin{bmatrix} \alpha_{1out} \\ \alpha_{2out} \end{bmatrix} = \frac{1}{\sqrt{2}} \begin{bmatrix} 1 & -i \\ -i & 1 \end{bmatrix} \begin{bmatrix} \alpha_{1in} \\ \alpha_{2in} \end{bmatrix} \tag{2.1.1}$$

where α_{1in} and α_{2in} are the complex amplitudes of two input fields and α_{1out} and α_{2out} are the complex amplitudes of two ouput fields as shown in Fig. (5).

The complex amplitudes of the two input fields can be expressed as $\alpha_{1in} = r_1 e^{i\theta_1}$ and $\alpha_{2in} = r_2 e^{i\theta_2}$. From the classical analysis, they determined the phase

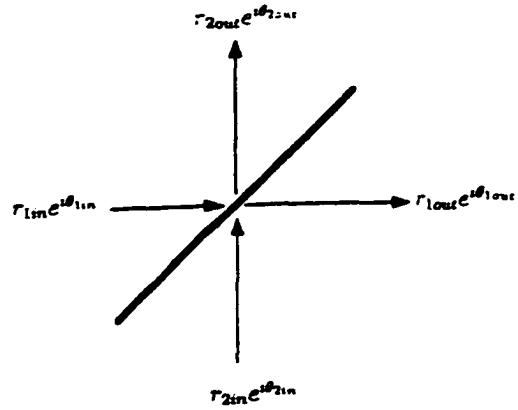

Figure 5: Classical analysis of the difference phase fluctuation of beam splitter output beams. It is assumed that the both r_1 and r_2 have the same mean value, $r = \langle r_1 \rangle = \langle r_2 \rangle$ and the mean value of $\theta_1 - \theta_2$ is zero. We define $\delta r_j = r_j - \langle r_j \rangle$ where $j = 1, 2$ and $\delta\theta_d = \theta_d - \langle \theta_d \rangle$.

difference of the two ouput fields,θ_d, in terms of parameters of the input field.

$$\theta_d = \arg(\alpha_{1out}\alpha^*_{2out}) = \arctan \frac{r_1^2 - r_2^2}{2r_1 r_2 \cos(\theta_1 - \theta_2)}. \tag{2.1.2}$$

We now need to discuss which branch of arctan should be taken. The quantity $2r_1 r_2 \cos(\theta_1 - \theta_2)$ is the real part of the $\alpha_{1out}\alpha^*_{2out}$. If the real part is positive, tangent fucntion is in either first quadrant or 4th quadrant and therefore the argument of $\alpha_{1out}\alpha^*_{2out}$ is between $-\pi/2$ and $\pi/2$. If the real part is negative, the tangent fucntion is either on 2nd quadrant or 3rd quadrant and the argument of $\alpha_{1out}\alpha^*_{2out}$ is between $\pi/2$ and π or between $-\pi$ and $-\pi/2$. So, if $\cos(\theta_1 - \theta_2) \geq 0$, then we have $-\pi/2 \leq \theta_d \leq \pi/2$. If the $\cos(\theta_1 - \theta_2) < 0$, then we have either $\pi/2 < \theta_d \leq \pi$ or $-\pi < \theta_d < -\pi/2$. If we consider the case of $r_1 = r_2 = r$,

θ_d is either zero or π depending whether $\cos(\theta_1 - \theta_2)$ is positive or negative: if $\cos(\theta_1 - \theta_2)$ is positive, θ_d is zero and if $\cos(\theta_1 - \theta_2)$ is negative, θ_d is π. If we include fluctuations, we can represent the phase angles of the input fields in terms of the mean values and fluctuations

$$\theta_1 = \langle\theta_1\rangle + \delta\theta_1 \tag{2.1.3}$$

$$\theta_2 = \langle\theta_2\rangle + \delta\theta_2. \tag{2.1.4}$$

Suppose the mean phase angles of the two input beam are equal. $\langle\theta_1\rangle = \langle\theta_2\rangle$. Then $\cos(\theta_1 - \theta_2)$ becomes $\cos(\delta\theta_1 - \delta\theta_2)$ cancelling out the mean phase anlgles of the input fields and if $-\frac{\pi}{2} < \delta\theta_1 - \delta\theta_2 < \frac{\pi}{2}$, then the phase difference of the two ouput beams is zero, $\theta_d = \langle\theta_d\rangle + \delta\theta d = 0$. In this case, we find the fluctuation of the phase difference of the ouput beam will be very small if the phase fluctuations of the input beams are less than $\frac{\pi}{4}$. $-\frac{\pi}{4} < \delta\theta_1 < \frac{\pi}{4}$ and $-\frac{\pi}{4} < \delta\theta_2 < \frac{\pi}{4}$. Thus one can obtain very small fluctuations of the difference phase of the ouput fields after the beam splitter even if there are substantial fluctuations of the phase in the input beam as long as the the magnitudes and the mean phases of the input fields are assumed to be the same. Such beams should be useful in the measurement of phase shifts in the interferometer.

The classical analysis by Hillery, Zou, and Buzek [10] provides good direction. By assuming small fluctuations in both amplitude and phase of the input fields, they showed that for two equal intensity input beams the noise in the phase

difference of the output depends only on the intensity noise of the input beams and not on their phase noise; a beam splitter turns reduced number state fluctuation into reduced difference phase noise

$$\langle(\delta\theta_d)^2\rangle = \frac{1}{r^2}\langle(\delta r_1 - \delta r_2)^2\rangle. \tag{2.1.5}$$

where δr_1 and δr_2 are intensity fluctuations of the input beams. This suggests that in the quantum case intensity squeezing could be converted to phase difference squeezing by a beam splitter. The most extreme case would be if $\delta r_1 = \delta r_2$. which classically, leads to no difference-phase noise at all.

2.2 Quantum squeezing

Following the classical analysis, we will investigate the effect of the intensity squeezing in the quantum case. For the purpose of utilizing Eq. (2.1.5), we are tempted to use number state as our input beams because there are no intensity fluctations, $\Delta n = 0$, in number state. However, the Heisenberg uncertainty principle $\Delta A \Delta B \geq \frac{1}{2}|\langle[A, B]\rangle|$ between the standard deviation of two arbitrary observables, $\Delta A = \sqrt{\langle(A - \langle A\rangle)^2}$ and similarly for ΔB, states that one can squeeze the standard deviation of one observables provided one stretches that for the conjugate observables. For example the position and momentum standard deviations or fluctuations obey the well known uncertainty relation

$$\Delta x \Delta p \geq \hbar/2 \tag{2.2.6}$$

If we try to reduce intensity fluctations, then we will increse the noise in another conjuage variable, the phase, according to the Heisenberg's uncertainty principle: for a number state where there are no intensity fluctuations, fluctuations in the phase are infinite. If we use two number states with equal intensities as the input fields for a beam splitter, then the phase difference for the output fields, θ_d, could be either zero or π and this point was well discussed in the paper by Hillery, Zou and Buzek [10]. We will discuss the number state input case and the related subjects in the next two chapters. We need a state where we can decrease the intensity fluctuaions and still have small fluctuations in phase. A general class of minimun uncertainty states known as squeezed states [18] meets our criterion. This squeezed state can be used to improve the sensitivity of the interferometer. As we have seen in the classical analysis, the decrease in the amplitude fluctuations of the input beams leads to the decrese in the phase difference fluctuation after the beam splitter. Thus, if we can send the beam squeezed in the direction of the amplitude, then we can increase the sensitivity of the interferometer.

For the single mode field, we may write the annihilation operator a as a linear combination of two Hermitian operators

$$a = X_1 + iX_2. \tag{2.2.7}$$

X_1 and X_2, the real and complex amplitude, give dimensionless amplitudes for the

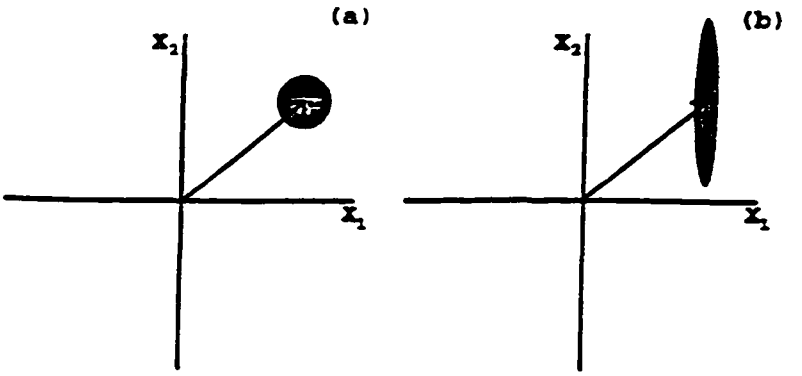

Figure 6: Phase-space plot showing the uncertainty in (a) a coherent state $|\alpha\rangle$, and (b) a squeezed state $|\alpha, r\rangle$.

mode's two quadrature phases. They obey the following commutation relation

$$[X_1, X_2] = i/2. \tag{2.2.8}$$

The corresponding uncertainty priciple is

$$\Delta X_1 \Delta X_2 \geq 1/4. \tag{2.2.9}$$

The coherent state state $|\alpha\rangle$ has the mean complex amplitude α and it is a minimum-uncertainty state for X_1 and X_2, with equal uncertainties in the two quadrature phases. A coherent state may be represented by an "error circle" in a complex amplitude plane whose axis are X_1 and X_2 (Fig. 6a). The center of the error circle lies at $\langle X_1 + iX_2 \rangle = \alpha$ and the radius $\Delta X_1 = \Delta X_2 = 1/2$ accounts for the uncertainties in X_1 and X_2.

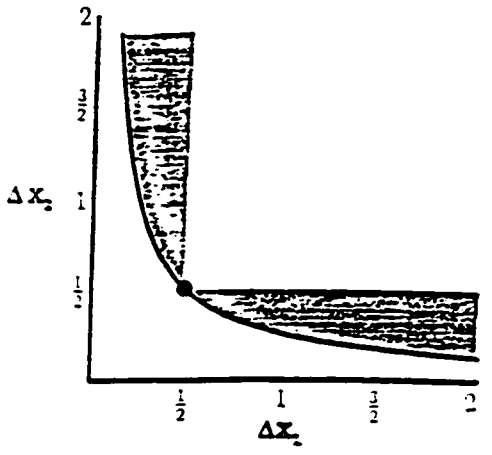

Figure 7: Plot of ΔX_1 versus ΔX_2 for the minimum-uncertainty states. The dot marks a coherent state while the shaded region corresponds to the squeezed states.

There is obviously a whole family of minimum-uncertainty states defined by $\Delta X_1 \Delta X_2 = 1/4$. If we plot ΔX_1 against ΔX_2, the minimum uncertainty states lie on a hyperbola (Fig. 7). Only points lying to the right of this hyperbola correspond to physical states. The coherent state with $\Delta X_1 = \Delta X_2$ is a special case of a more general class of states which may have reduced uncertainty in one quadruture at the expense of increased uncertainty in the other. These states, called squeezed states [18], can be used to improve the accuracy of interferometric measurements, and to reduce quantum noise in measurements in general. Formally, we can generate such a state by using the squeeze operator [19]

$$S(z) = e^{\frac{1}{2}(za^{\dagger 2} - z^* a^2)} \tag{2.2.10}$$

which acts as follows:

$$S^{\dagger}(z)aS(z) = a\cosh r + a^{\dagger}e^{i\theta}\sinh r \tag{2.2.11}$$

$$S^{\dagger}(z)a^{\dagger}S(z) = a^{\dagger}\cosh r + ae^{-i\theta}\sinh r \tag{2.2.12}$$

where $z = re^{i\theta}$. The squeeze operator attenuates one component of the complex amplitude, and it amplifies the other component. The degree of attenuation and amplification is determined by r, which we called the squeeze factor. The squeezing parameter $z = re^{i\theta}$ also contains the phasor θ which controls the direction of the squeezing in the phase space: if we calculate $\Delta X_1 = \sqrt{\langle X_1^2\rangle - \langle X_1\rangle^2}$ and $\Delta X_2 = \sqrt{\langle X_2^2\rangle - \langle X_2\rangle^2}$ for a squeezed vacuum, $S(z)|0\rangle$, we have

$$\Delta X_1 = \frac{1}{2}\sqrt{2\sinh r^2 + 1 + 2\cosh r\sinh r\cos\theta} \tag{2.2.13}$$

$$\Delta X_2 = \frac{1}{2}\sqrt{2\sinh r^2 + 1 - 2\cosh r\sinh r\cos\theta}. \tag{2.2.14}$$

For $\theta = 0$ we have $\Delta X_1 = \frac{1}{2}e^{r}$ and $\Delta X_2 = \frac{1}{2}e^{-r}$. In this case we have X_2 quadrature squeezed and fluctuations in X_1 have increased to satisfy the Heisenberg's uncertainty priciple. For a vacuum state without any squeezing, we have $\Delta X_1 = \Delta X_2 = 1/2$. We can also state that the X_1 operator has been transformed as $e^{r}X_1$ and X_2 operator as $e^{-r}X_2$. For $\theta = \pi$, then X_1 quadruture is squeezed and X_2 quadruture is amplified; $\Delta X_1 = \frac{1}{2}e^{-r}$ and $\Delta X_2 = \frac{1}{2}e^{r}$.

For a squeezed-coherent state, we squeeze the vacuum first and then displace it. The squeezed-coherent state is formally obtained by

$$|\alpha, z\rangle = D(\alpha)S(z)|0\rangle \tag{2.2.15}$$

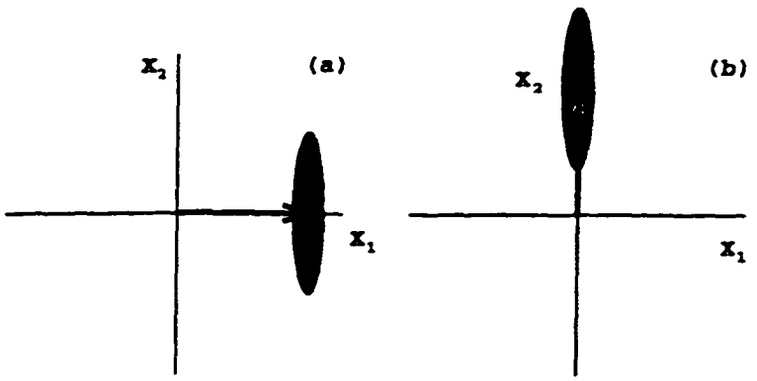

Figure 8: Phase-space representation of amplitude and phase squeezed states. (a) The quadruture carrying the coherent excitation is squeezed. (b) The quadruture out of phase with the coherent excitation is squeezed.

where

$$D(\alpha) = e^{(-\alpha a^{\dagger} + \alpha^{*} a)}. \tag{2.2.16}$$

If we displace along with the direction of the squeezing (Fig. 8a), then we have the effect of the squeezing the amplitude ; for example, if we have α as real number and the direction of the squeezing is π, then we are squeezing the X_1 quadrature and therefore we are squeezing fluctution in α . $|\alpha|^2$ is the mean number of photons in the field and therefore, we are squeezing the amplitude of the field. On the other hand if the direction of the squeezing is out of the phase with the coherent excitation , we have squeezing in the phase and thus, increased in noise of the amplitude (Fig. 8b).

2.3 Squeezed states and the phase shift measurements

As discussed in the classical analysis, beam splitter turns reduced fluctuations in intensity of the input beams into difference phase squeezing; a peak in the difference phase distriubution will become narrower for the intensity squeezed state input beams. Therefore, the squeezed-coherent states we choose for input states are both squeezed and displaced along the x-axis (Fig. 8a). The complex amplitude is then real and the squeezing is such that it is in magnitude of the complex amplitude: it is the intensity fluctuations which are squeezed. We assume amplitudes of the two input beams to be the same, $\alpha_1 = \alpha_2 = \alpha$. In this squeezed-coherent state with the squeezing in phase with the complex amplitude, we have

$$V(n) = |\alpha|^2 e^{-2r} + 2\sinh^2[r]\cosh^2[r] \tag{2.3.17}$$

where $V(n)$ is the variance in the photon number, $V(n) = \langle (aa^\dagger)^2 \rangle - \langle aa^\dagger \rangle^2$. The first term corresponds to the reduction in number fluctuation in the original Poisson distribution. The second term is due to the fluctuation of the additional photons in the squeezed vacuum. In this squeezed-coherent state, the amplitude fluctuation is "squeezed" if the squeezing factor,r, becomes large but not large enough so that the second term becomes dominant. It then behaves more like a number state where the amplitude fluctuation, $\Delta n = 0$. For example if $|\alpha|^2 \gg 2\sinh^2 r \cosh^2 r$, this is an amplitude squeezed state with sub-Poissonian photon statistics. The maximum reduction in photon number fluctuations one can get

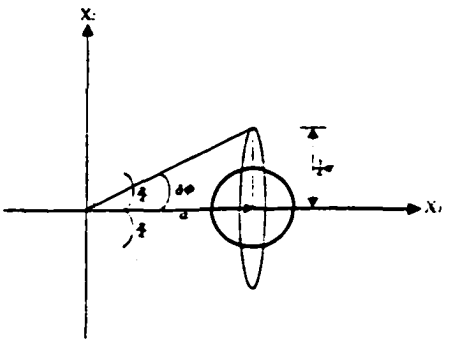

Figure 9: Phase fluctuations in the squeezed-coherent state: δo gets bigger as the squeezing increases.

in an amplitude squeezed state may be estimated as follows: For $r \geq 1$

$$V(n) \approx |\alpha|^2 e^{-2r} + \frac{1}{8} e^{4r} \tag{2.3.18}$$

The minimum value of $V(n)$ occurs for $e^{6r} = 4|\alpha|^2$ which corresponds to $V_{min}(n) \approx 0.94|\alpha|^{4/3}$. The maximum intensity squeezing occurs for $r = \frac{1}{6}\ln(4|\alpha|^2)$. As shown in Fig. (9), as we increase the intensity squeezing, X_1 quadrature components becomes smaller and X_2 quadrature component becomes bigger. The phase fluctuation of the input beams.$\tan(\delta o) = \frac{e^r}{2\alpha}$. also becomes larger. Now the minimum phase that can be detected using squeezed-coherent states with decreased amplitude fluctuation is calculated

$$\begin{aligned} \delta o_{min} &= \Delta J_{3\text{out}} / \left| \frac{d\langle J_{3\text{out}}\rangle}{do} \right| \\ &= \left(\frac{2\sqrt{p}}{8\alpha^4}\right)^{\frac{1}{2}} = \frac{1}{2\alpha^2} p^{\frac{1}{4}}. \end{aligned} \tag{2.3.19}$$

where

$$
\begin{aligned}
p \;=\; & 16\cosh^6[r]\sinh^2[r] + 96\cosh^4[r]\sinh^4[4] \\
& + 16\cosh^2[r]\sinh^6[r] \\
& + \alpha^2\left\{2\cosh^6[r] - 28\cosh^5[r]\sinh[r]\right. \\
& + 126\cosh^4[r]\sinh^2[r] - 200\cosh^3[r]\sinh^3[r] \\
& \left.+126\cosh^2[r]\sinh^4[r] - 28\cosh[r]\sinh^5[r] + 2\sinh^6[r]\right\} \\
& \alpha^4\left\{8\cosh^4[r] - 32\cosh^3[r]\sinh[r]\right. \\
& + 48\cosh^4[r]\sinh^2[r] - 32\cosh^2[r]\sinh^2[r] \\
& \left.-32\cosh[r]\sinh^3[r] + 8\sinh^4[r]\right\} \qquad (2.3.20)
\end{aligned}
$$

For the $\delta\phi$ for squeezed-coherent state input is in the order of $1/\alpha$ when there is no squeezing. coherent state. Thus. the minimum detectable phase shift for a squeezed-coherent state works in the limiting case. In Fig.10 and Fig. 11. we have plotted the $\Delta(n_1 - n_2)^2$ and the minimum detectable phase angle.$\delta\phi$ as functions of the squeezing parameter.r. As expected. the sensitivity of the interferometer gets better as the squeezing gets larger and larger until the maximum intensity squeezing. After the squeezing parameter reaches maximum point. the sensitivity deteriorates. Also, $\Delta(n_1 - n_2)^2$ behaves the exactly same way as $\delta\phi$. And these confirm the classical analysis that difference phase squeezing is achieved from the amplitude squeezing if the amplitude squeezing is not too big and this enhances the sensitivity of the interferometer.

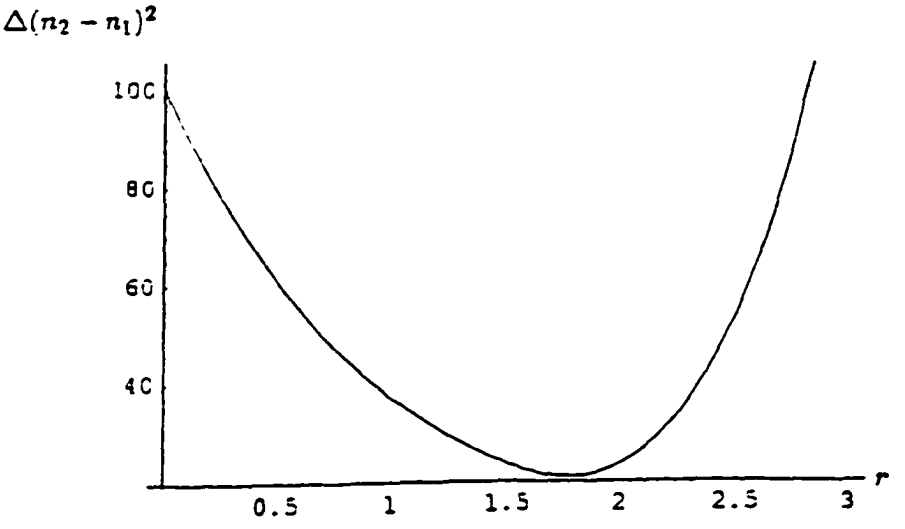

Figure 10: Plot of $\Delta(n_2 - n_1)^2$ versus r when a is 100

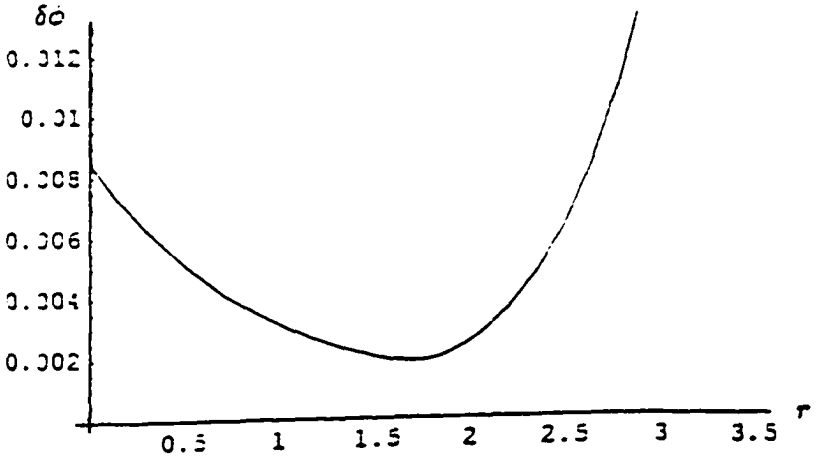

Figure 11: Plot of δo versus r when a is 100

Chapter III

3 Number state inputs

3.1 Introduction

A number state is a state with no intensity fluctuations but with arbitrary phase, an obvious consequence of Heisenberg's uncertainty priciple. We choose to have two number states as our input beams to the interferometer: two input states with no intensity fluctuations and equal intensities. Classically, from equation (2.1.2)

$$\theta_d = \arg(\alpha_{1out}\alpha_{2out}^*) = \arctan\frac{r_1^2 - r_2^2}{2r_1 r_2 \cos(\theta_1 - \theta_2)}.$$

we see that for number state inputs the $\cos(\theta_1 - \theta_2)$ term in the denominator can be positive or negative because the phase of a number state is arbitrary. This indicates that the phase of the output state after the first beam splitter in the interferometer but before going through a phase shift can be either 0 or π for the two number states with the equal intensities. Quantum mechanically, Hillery, Zou and Buzek [10] showed that the difference phase distribution of the output beams for the two number state inputs consists of two narrow peaks centered around at $\theta = 0$ and $\theta = \pi$; the output state after the beam splitter is a superposition of a state with a difference phase of 0 and another with a difference phase of

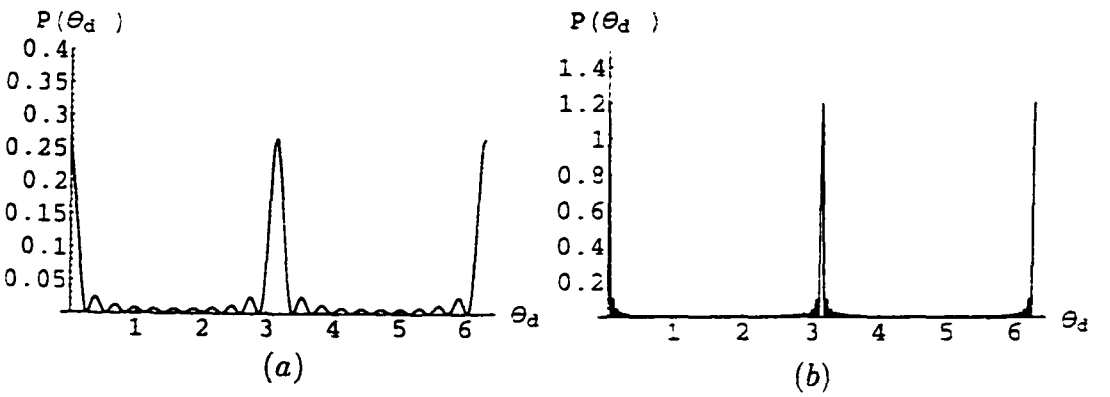

Figure 12: The difference phase distribution for number state inputs with equal intensities. $|n, n\rangle$: a) n=10 case b) n=50.

π. This is shown in Fig. (12). This double peak structure of difference phase distribution after the first beam splitter inside the interferometer causes the output signal of the interferometer to vanish. What is measured at the output of the interferometer is the photon number differences . $\langle \text{out}|J_3|\text{out}\rangle$ where $|\text{out}\rangle$ is the state of the photon field leaving the interferometer. From the equation (1.5.104), we have for the number state inputs

$$\begin{aligned} \langle J_{3\text{out}}\rangle &= \langle \text{out}|J_{3\text{in}}|\text{out}\rangle \\ &= -\sin\phi\langle \text{in}|J_{1\text{in}}|\text{in}\rangle + \cos\phi\langle \text{in}|J_{3\text{in}}|\text{in}\rangle \\ &= \frac{1}{2}\cos\phi(n_1 - n_2) \end{aligned} \tag{3.1.1}$$

where n_1 and n_2 are the photon numbers at each input ports of the interferometer.

For input beams with equal intensities, $n_1 = n_2$, the expectation value of J_3 is zero; the mean number of photons counted at the two outputs is same and therefore, the signal coming from measuring the photon number differences will vanish. Equation (3.1.1) shows that the $\langle J_{3\text{out}} \rangle$ is independent of ϕ for the input beams with equal intensities. Changes in $\delta\phi$ in the phase angle are detected by the changes they create in the expectation of J_3. Therefore, the phase shift introduced in the inteferometer does not induce any changes in the expectation value of $J_{3\text{out}}$ for the two number state input beams with the equal intensities and consequently, we cannot measure the phase shift introduced in the interferometer.

We have calculated the minimum detectable phase shift for the general number state input $|n_1, n_2\rangle$

$$\begin{aligned} \delta o &= \Delta J_{3out} / \; d\langle \frac{J_{3out}}{do} \rangle \\ &= \frac{\sqrt{n + \frac{1}{2}(n^2 - x^2)}}{x} \end{aligned} \tag{3.1.2}$$

where $n = n_1 + n_2$ is the total number of photons for the incoming fields and $x = n_1 - n_2$ is the photon number difference between the two input ports. The minimum detectable phase shift for these states is $1/\sqrt{n}$ when $x = n$: the case when we have vaccum state in one of the input ports and n photons in the other input port. As disccussed above, the minimum detectable phase shift is undefined as x approaches zero (see Fig. 13); the case when we have two number state inputs with equal intensities. We also notice that the sensitivity of the interferometer

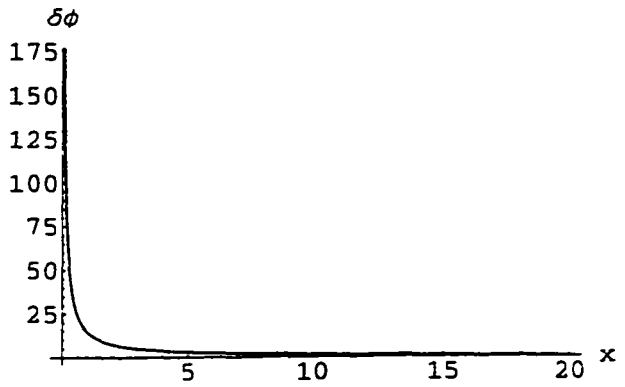

Figure 13: Minimum detectable phase shift for number state inputs, $|n_1, n_2\rangle$, as a function of photon number difference. $x = n_1 - n_2$

deteriorates from the case when we have vaccum state in one of the input port as soon as there is beam coming in the second input port.

We can interpret the above analysis in a different way. Since we have from the equation (1.5.89)

$$\langle \text{out}|J_3|\text{out}\rangle = \langle \text{intermediate}|J_2|\text{intermediate}\rangle. \tag{3.1.3}$$

measuring the photon number differences at the output ports is equivalent to evaluate the expectation value of J_2, $\langle \text{intermediate}|J_2|\text{intermediate}\rangle$ where $|\text{intermediate}\rangle$ is the state of the photon field after going through a phase shift inside the interferometer. We find the classically corresponding quantity for J_2 by replacing a_1 and a_2 by $r_1 e^{i\theta_1}$ and $r_2 e^{i\theta_2}$ respectively,

$$J_2 = -i(a_1^\dagger a_2 - a_1 a_2^\dagger)/2 \quad \Leftrightarrow \quad -i\frac{1}{2}(r_1 r_2)(e^{-i(\theta_1-\theta_2)} - e^{i(\theta_1-\theta_2)})$$

$$= \quad -r_1 r_2 \sin(\theta_1 - \theta_2) \tag{3.1.4}$$

By comparing the equation (3.1.3) and the equation (3.1.4), we find that measurement of the photon number differences reveals implicitly the phase information inside the interferometer. Alternatively, we can say that the phase distribution after the first beam spitter determines the sensitivity of the interferometer. The narrower the difference phase ditsribution peak, the smaller the minimum detectable phase shift.

After the first beam splitter but before going through the phase shift, the difference phase distribution for the two number states with the equal intensities has peaks at 0 and π shown in Fig. (14). Now one of the beams goes through a phase shift, ϕ, and this shifts the two peaks of the difference phase distribtution by ϕ as shown in Fig. (14). The measurment of J_3 at the output ports is equivalent to measurement of J_2 for the fields just before the second beam splitter, and J_2 classically corresponds to $-\sin(\theta_1 - \theta_2)$. Therefore, measuring the expectation value of J_2 is classically equivalelnt to calculating $r_1 r_2 \int_0^{2\pi} P(\theta_d) \sin\theta_d \, d\theta_d$ where $P(\theta_d)$ is the difference phase distribution for the beams inside the inteferometer after the phase shift is introduced into one of the legs.

For number states with large numbers of photons the peaks at zero and π are very narrow. The rotational width is proportional to $1/N$ where N is the number of photons going into the interferometer [4]. The rotational width is derived from

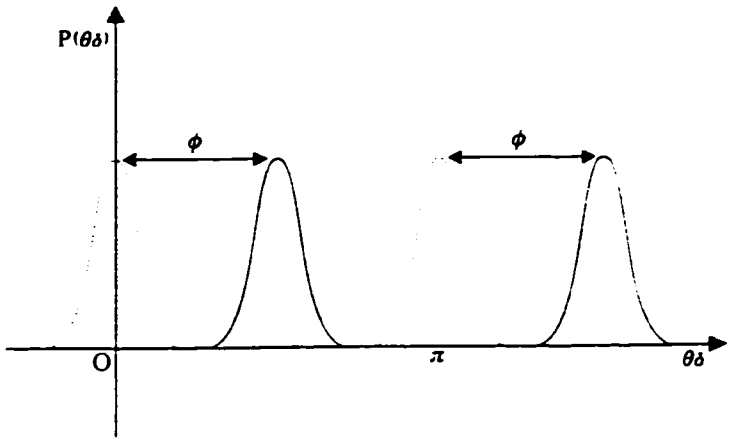

Figure 14: The differece phase distribution for two number state inputs with equal intensities after the first beam splitter (dotted line) and the difference phase distribution after the phase shift introdued in one of the leg (solid line).

examining the overlap between a state and a rotated version of itself. It gives a good indication of the utility of a state for measuring phase shifts . In the case of the difference phase we can determine the rotational width by considering the function

$$F(\theta_d) = |\langle \upsilon | e^{-i\theta_d J_3} \upsilon \rangle|^2. \tag{3.1.5}$$

This function has a maximum value of one for $\theta_d = 0$ and near this peak it is peak is given by

$$F(\theta_d) \cong 1 - (\triangle J_3)^2 \theta_d^2. \tag{3.1.6}$$

From this Hillery, Buzek and Zou [4] deterimed the rotational width for the number state input beam with equal intensities from the equation (3.1.6).

If the number of input photons is reasonably large, we can roughly represent the phase difference distribution as a sum of dirac-delta functions, $P(\theta_d) = \frac{1}{2}(\delta(\theta_d) + \delta(\theta_d - \pi))$. The classical equivalent of the expectation value of J_2 after the first beam splitter is

$$\begin{aligned} r^2 \int_0^{2\pi} P(\theta_d) \sin\theta_d d\theta_d &= r^2 \int_0^{2\pi} \frac{1}{2}(\delta(\theta_d) + \delta(\theta_d - \pi)) \sin\theta_d d\theta_d \\ &= \frac{1}{2} r^2 (\sin(0) + \sin(\pi)) = 0 \end{aligned} \tag{3.1.7}$$

The above classical equivalent is zero even for the case of a difference phase distribution which has only a peak either at zero or π. because the sine functioin is zero at zero and π. After the beams go through the phase shifter. if there is only one peak at either at zero or at π, the integration is not zero because the difference phase distribtion is now shifted by the amount of ϕ. For example. for the case of two coherent state input beams with the same mean photon numbers. we have a difference phase distribution peaked at zero after the first beam splitter. After the phase shift.ϕ, we have

$$\begin{aligned} r^2 \int_0^{2\pi} P(\theta_d) \sin\theta_d d\theta_d &= r^2 \int_0^{2\pi} \delta(\theta_d - \phi) \sin\theta_d d\theta_d \\ &= r^2 \sin(\phi). \end{aligned} \tag{3.1.8}$$

Therefore, for the case of two coherent state input beams, the phase shift inside the interferometer will create changes in the expectation value of J_3. However, if we have two peaks located at zero and π, then the contributions to the integral from two shifted peaks cancel each other, and therefore the integral is zero. For

the number state input with the equal intensity, we have

$$\begin{aligned} r^2 \int_0^{2\pi} P(\theta_d) \sin\theta_d d\theta_d &= r^2 \int_0^{2\pi} \frac{1}{2}(\delta(\theta_d - \phi) + \delta(\theta_d - \phi - \pi)) \sin\theta_d d\theta_d \\ &= \frac{1}{2} r^2 (\sin(\phi) + \sin(\pi + \phi)) \\ &= \frac{1}{2} r^2 (\sin(\phi) - \sin(\phi)) \\ &= 0. \end{aligned} \tag{3.1.9}$$

This analysis shows that the signal coming from the expectation value of J_3 is zero, and we can not measure the phase shift by measuring the mean photon number differences at the output ports of the interferometer. This is unfortunate because the peaks are very narrow, having rotational widths of $1/N$. It is a much narrower width than the case for the two coherent state inputs with the same amplitudes. In that case the difference phase distribution after the beam splitter is peaked at zero with the width of the peak being of order of $1/\sqrt{N}$.

In order to circumvent the difficulties for the detection of phase shift introduced inside the interferometer by measuring the photon number differences at the output ports of the interferometer, $\langle J_3 \rangle$, we examined the possibility of using the expectation value of J_3^2 instead of J_3. While there is no signal when we measure the expectation vaule of J_3, there will be signal when we measure the expectation value of J_3^2. However, signal to noise ratio for this measurement is poor. From the equation (1.5.104), we have

$$J_{3\text{out}} = -J_1 \sin\phi + J_3 \cos\phi.$$

If we take the expectation value of J_{3out} in the two mode number state with equal intensities, then we have

$$\langle n, n|J_{3out}|n, n\rangle = 0. \tag{3.1.10}$$

If we square the J_{3out}, then we have

$$(J_{3out})^2 = J_1^2 \sin^2\phi - (J_1J_3 + J_3J_1)\cos\phi\sin\phi + J_3^2\cos^2\phi \tag{3.1.11}$$

From the above equation, the only term that will give a contribution when we take the expectation value of J_3^2 in the two mode number state with the equal intensities, $|n, n\rangle$, is J_1^2. J_1J_3 and J_3J_1 will give no contribution because the number of creation and annhilation opearators is unequal. J_3^2 term will give no contribution either because $J_3|n, n\rangle = 0$. Therefore, we have for the expectation value of J_3^2

$$\begin{aligned}
\langle (J_{3out})^2\rangle &= \langle J_1^2\rangle \sin^2\phi \\
&= \frac{1}{4}\langle n, n|(a_1^\dagger a_2 + a_1 a_2^\dagger)(a_1^\dagger a_2 + a_1 a_2^\dagger)|n, n\rangle \sin^2\phi \\
&= \frac{1}{4}\langle n, n|a_1^\dagger a_1 a_2 a_2^\dagger + a_1 a_1^\dagger a_2^\dagger a_2|n, n\rangle \sin^2\phi \\
&= \frac{1}{2}n(n+1)\sin^2\phi.
\end{aligned} \tag{3.1.12}$$

Now we need to calculate $\Delta(J_{3out}^2)$ to see how big the noise is . We have $\Delta(J_{3out}^2) = \sqrt{\langle J_{3out}^4\rangle - \langle J_{3out}^2\rangle^2}$. There are 16 terms when we take the fourth power of the equation (1.5.104) to calculate the $\langle J_{3out}^4\rangle$. Out of those 16 terms, anything with J_3 on the outside will give zero and we have

$$\langle J_{3out}^4\rangle = \langle (J_1\sin\phi)(-J_1\sin\phi + J_3\cos\phi)(-J_1\sin\phi + J_3\cos\phi)(J_1\sin\phi)\rangle. \tag{3.1.13}$$

There are four terms in the equation (3.1.13) and among them two terms will not contribute to the expectation value of J_{3out}^4; terms of the form $J_1^2 J_3 J_1$ and $J_1 J_3 J_1^4$ have unbalanced numbers of J_+'s and J_-'s and therefore, they will give no contribution. For the expectation value of J_1^4, we have

$$\begin{aligned}\langle J_1^4\rangle &= \frac{1}{16}\langle n.n|(a_1^\dagger a_2 + a_1 a_2^\dagger)^4|n.n\rangle \\ &= \frac{1}{8}[n(n-1)(n+1)(n+2) + 2n^2(n+1)^2]\sin^2\phi \qquad (3.1.14)\end{aligned}$$

and we also have for the expectation value of $J_1 J_3^2 J_1$

$$\begin{aligned}\langle J_1 J_3^2 J_1\rangle &= \frac{1}{4}\langle n.n|J_1 J_3^2 J_1|n.n\rangle \\ &= \frac{1}{2}n(n+1) \qquad (3.1.15)\end{aligned}$$

Using the equation (3.1.12), (3.1.14) and (3.1.15), we obtain the dispersion of J_{3out}^2

$$\begin{aligned}\Delta(J_{3out}^2) &= \sqrt{\langle J_{3out}^4\rangle - \langle J_{3out}^2\rangle^2} \\ &= \{\frac{1}{8}[n(n-1)(n+1)(n+2) + 2n^2(n+1)^2]\sin^4\phi \\ &\quad + \frac{1}{2}[n(n+1)]\sin^2\phi\cos^2\phi - \frac{1}{4}[n^2(n+1)^2]\sin^4\phi\}^{\frac{1}{2}} \\ &= \{\frac{1}{8}[n(n-1)(n+1)(n+2)]\sin^4\phi + \frac{1}{2}[n(n+1)]\sin^2\phi\cos^2\phi\}^{\frac{1}{2}} \qquad (3.1.16)\end{aligned}$$

From the equation (3.1.12) and (3.1.16) we have for large numbers of photons

$$\Delta J_{3out}^2 = \frac{n^2}{2\sqrt{2}}\sin^2(\phi) \qquad (3.1.17)$$

$$\langle (J_{3out})^2\rangle = \frac{1}{2}n^2\sin^2(\phi). \qquad (3.1.18)$$

Noise increases just as fast as the signal and their ratio is order of 1. This is disappointing because we obtain our signal by measuring J_{3out}^2. This means that by measuring the expectation value of J_3^2 we will not be able to accurately measure the phase shift. This was also proved independently by other group [22].

3.2 A number state and a vaccum state as input beams

So far we have considered the case of two number state inputs with equal intensities, $|n, n\rangle$. When n photons are sent into one of two input ports of the interferometer and a vaccum state is sent into the second input port. the minumum detectable phase shift.$\delta\phi$, is $1/\sqrt{n}$ where n is the number of photons entering into the interferometer. This is the same as the case when a coherent state and a vaccum state are sent into the input ports of the interferometer. In this case, n is the mean number of photons in the input state. This sensitivity can be explained in terms of the difference phase distribution after the first beam splitter inside the interferometer. In Fig (15), we present a numerical simulation of the difference phase distribution for the input state $|n, 0\rangle$. The difference phase distribution has a peak at $\theta_d = \pi/2$. Here in this case, there is only one peak and therefore, rotational width of the difference phase distribution will determine the sensitivity of the interferometer.

We would like to calculate $\langle\theta_1, \theta_2|U_1|n, 0\rangle$. The output state after the first

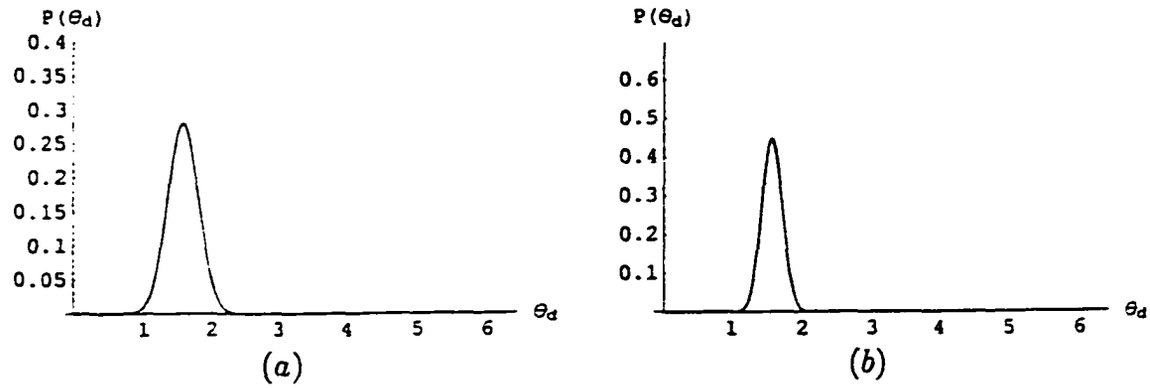

Figure 15: The computer-simulation of the difference phase distribution for a) $|20.0\rangle$ input state and b) $|50,0\rangle$ input state.

beam splitter insider the interferometer is

$$\begin{aligned} |\psi_{\text{out}}\rangle = U_1|\psi_{\text{in}}\rangle &= e^{-i\phi J_1}|n,0\rangle \\ &= e^{-i\phi J_1}\frac{(a_1^\dagger)^n}{\sqrt{n!}}|0,0\rangle \\ &= e^{-i\phi J_1}\frac{(a_1^\dagger)^n}{\sqrt{n!}}e^{i\phi J_1}|0,0\rangle \end{aligned} \tag{3.2.19}$$

where we have used $e^{i\phi J_1}|0,0\rangle = |0,0\rangle$. Using $U_1 a_1^\dagger U_1^{-1} = \frac{1}{\sqrt{2}}(a_1^\dagger - ia_2^\dagger)$, equation (3.2.19) becomes

$$\begin{aligned} |\psi_{\text{out}}\rangle &= \frac{1}{\sqrt{n!}}(\frac{1}{\sqrt{2}})^n(a_1^\dagger - ia_2^\dagger)^n|0,0\rangle \\ &= (\frac{1}{\sqrt{2}})^n\sum_{l=0}^{n}\frac{\sqrt{n!}}{\sqrt{l!(n-l)!}}(-i)^{(n-l)}|l,n-l\rangle. \end{aligned} \tag{3.2.20}$$

We now have

$$\langle\theta_1,\theta_2|\psi_{\text{out}}\rangle = (\frac{1}{\sqrt{2}})^n e^{-in\theta_2}(-i)^n \sum_{l=0}^{n} \frac{\sqrt{n!}}{\sqrt{l!(n-l)!}} e^{-il(\theta_1-\theta_2-\frac{\pi}{2})}. \tag{3.2.21}$$

We would like to approximate the following for a large value of n

$$f(l) = \frac{n!}{l!(n-l)!}. \tag{3.2.22}$$

Using the Sterling's approximation. $\ln(n!) \approx n\ln n - n$. we have for equation (3.2.22)

$$g(l) = \ln f(l) = \ln \frac{n!}{l!(n-l)!} \approx n\ln n - l\ln l - (n-l)\ln(n-l). \tag{3.2.23}$$

Differentiating the equation (3.2.23) with respect to l and setting it equal to zero. we obtain

$$\frac{d}{dl}g(l) \approx -\ln l + \ln(n-l) = 0. \tag{3.2.24}$$

From equation (3.2.24) . we find that when $l = \frac{n}{2}$. the function $g(l)$ is at its maximum value. We then do a Taylor series expansion about $l = \frac{n}{2}$ up to the second order

$$g(l) = g(\frac{n}{2}) + (l-\frac{n}{2})g'(\frac{n}{2}) + \frac{(l-\frac{n}{2})^2}{2!}g''(\frac{n}{2}). \tag{3.2.25}$$

We now have

$$g(l) = \ln f(l) = \ln(\frac{n!}{l!(n-l)!}) \approx \ln(\frac{n!}{(\frac{n}{2}!)(\frac{n}{2}!)}) + \frac{(l-\frac{n}{2})^2}{2}(-\frac{4}{n}). \tag{3.2.26}$$

Using the Sterling's approximation again including the next highest term.$\ln(n)! \approx n\ln n - z + \ln(\sqrt{2\pi n})$ we have for the first term on the right-hand side equation

(3.2.26).

$$\ln(\frac{n!}{(\frac{n}{2}!)(\frac{n}{2}!)}) \approx \ln(2^n\sqrt{\frac{2}{\pi n}}). \tag{3.2.27}$$

Substituting $\ln(2^n\sqrt{\frac{2}{\pi n}})$ for $\ln(\frac{n!}{(\frac{n}{2}!)(\frac{n}{2}!)})$ in the equation (3.2.26), we have

$$\ln(\frac{n!}{l!(n-l)!}) = \ln 2^n\sqrt{\frac{2}{\pi n}} - \frac{2}{n}(l-\frac{n}{2})^2. \tag{3.2.28}$$

Therefore, we have

$$\frac{n!}{l!(n-l)!} = (2)^n\sqrt{\frac{2}{\pi n}}e^{-\frac{2}{n}(l-\frac{n}{2})^2} \tag{3.2.29}$$

and

$$\sqrt{\frac{n!}{l!(n-l)!}} = (2)^{\frac{n}{2}}(\frac{2}{\pi n})^{\frac{1}{4}}e^{-\frac{1}{n}(l-\frac{n}{2})^2}. \tag{3.2.30}$$

With equation (3.2.30), equation (3.2.19) becomes

$$\langle\theta_1,\theta_2|v_{\text{out}}\rangle = (\frac{1}{\sqrt{2}})^n(2)^{\frac{n}{2}}(\frac{2}{\pi n})^{\frac{1}{4}}e^{-in\theta_2}(-i)^n\sum_{l=0}^{n}e^{-\frac{1}{n}(l-\frac{n}{2})^2}e^{-il(\theta_d-\frac{\pi}{2})} \tag{3.2.31}$$

where $\theta_d = \theta_1 - \theta_2$. Now we would like to replace the summation in the equation (3.2.31) by an integration

$$\sum_{l=0}^{n}e^{-\frac{1}{n}(l-\frac{n}{2})^2}e^{-il\beta} \approx \int_{-\infty}^{\infty}dl\,e^{-\frac{1}{n}(l-\frac{n}{2})^2}e^{-il\beta} \tag{3.2.32}$$

where $\beta = \theta_d - \frac{\pi}{2}$. The replacement of the summation by an integration is justified only when β is small. The integrand in equation (3.2.32) is $e^{-i\beta l}$ times a Guassian whose width is $\sqrt{n}$ and whose peak is located at $l = \frac{n}{2}$. As long as the oscillating function $e^{-i\beta l}$ changes little across the peak, then the going from a summation to an integration for approximation is justified and therefore, we require that $\beta\sqrt{n} \ll 1$. Therefore, the approximation should be good for all values of β; it is

good when $\beta \ll \frac{1}{\sqrt{n}}$ where distribution is large and is not good when distribution is negligible. If we perform the integration, then the integration becomes

$$\int_{-\infty}^{\infty} dl\, e^{-\frac{1}{n}(l-\frac{n}{2})^2} e^{-il\beta} = (\sqrt{\pi n}) e^{-i\beta\frac{n}{2}} e^{-\frac{n}{4}\beta^2} \tag{3.2.33}$$

Putting everything together, the equation (3.2.19) becomes

$$\langle \theta_1, \theta_2 | \psi_{\text{out}} \rangle = (\frac{1}{\sqrt{2}})^n (2)^{\frac{n}{2}} e^{-in\theta_2} (-i)^n (\frac{2}{\pi n})^{\frac{1}{4}} (\sqrt{\pi n}) e^{-i\beta\frac{n}{2}} e^{-\frac{n}{4}\beta^2}. \tag{3.2.34}$$

For large numbers of photons, we now have the difference phase distribution for the input state, $|n, 0\rangle$

$$\begin{aligned} P(\theta_1, \theta_2) &= \frac{1}{4\pi^2} |\langle \theta_1, \theta_2 | \psi_{\text{out}} \rangle|^2 \\ &= \frac{1}{4\pi^2} \sqrt{2\pi n}\, e^{-\frac{n}{2}(\theta_d - \frac{\pi}{2})^2} \,. \theta_d = \theta_1 - \theta_2. \end{aligned} \tag{3.2.35}$$

From this equation, we see that the analytical analysis agrees with the numerical simulation. They both show that the the difference phase distribution is peaked around $\frac{\pi}{2}$. From the equation (3.1.37), we find that the rotational width is in the order of $\frac{1}{\sqrt{n}}$ and this explains why the sensitivity of the inferometer for the input state $|n, 0\rangle$ is in the order of $\frac{1}{\sqrt{n}}$. Here we again showed the relation of the difference phase distribution to the sensitivity of the interferometer: the narrower the rotational width, the more sensitive the interferometer.

3.3 N photons and one photon as input beams

Now we like to consider the case when there is one photon coming in the one of

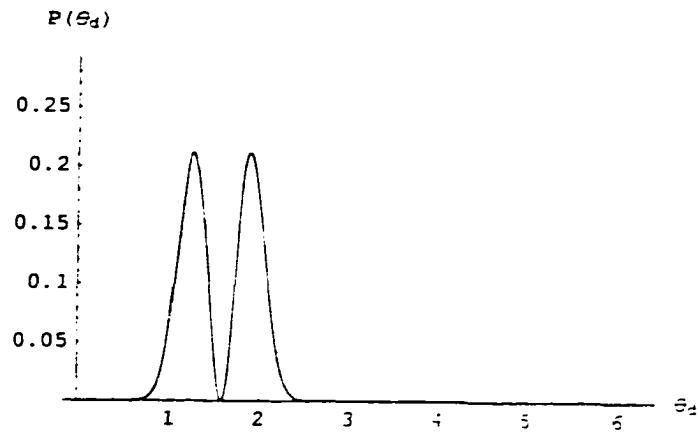

Figure 16: The computer-simulation of the difference phase distribution for $|20, 1\rangle$ input state.

the input ports instead of the vaccum state, $|n, 1\rangle$. From the equation (3.1.2), we have noted before that the sensitivity of the interferometer deteriorates as soon as there is beam coming in instead of vaccum state. For this input state $|n, 1\rangle$, the minimum detectable angle is $\delta\phi = \frac{\sqrt{3}}{\sqrt{n}}$ for large enough input photons. This deterioration comes not from the rotational width but from the cancellation of the signal as in the case of the two input states with the equal intensities. Actually, the rotational width of the difference distribution is in the order of $1/n$ for each of the peaks centered at 0 and π. From the numerical analysis shown in the Fig (16), there are two peaks for the difference phase distribution. It looks as though the one photon splits the phase difference distribution and shifts the peaks left and right symmetrically from $\frac{\pi}{2}$. As soon as there is one photon in the input port, two

peaks shows up spontaeneouly. This two-peak structure causes the deterioration of the sensitivity of the interferometer. We wish to calculate $\langle\theta_1,\theta_2|U_1|n,1\rangle$.The output state after the the first beam splitter inside the interferometer is

$$\begin{aligned}|\psi_{\rm out}\rangle = U_1|\psi_{\rm in}\rangle &= e^{-i\phi J_1}|n.1\rangle \\ &= e^{-i\phi J_1}\frac{(a_1^\dagger)^n}{\sqrt{n!}}(a_2^\dagger)|0.0,\rangle \\ &= e^{-i\phi J_1}\frac{(a_1^\dagger)^n}{\sqrt{n!}}(a_2^\dagger)e^{i\phi J_1}|0.0.\rangle. \end{aligned} \tag{3.3.36}$$

Using $U_1 a_1^\dagger U_1^{-1} = (ca_1^\dagger + sa_2^\dagger)$ and $U_1 a_2^\dagger U_1^{-1} = (sa_1^\dagger + ca_2^\dagger)$ where $c = \frac{1}{\sqrt{2}}$ and $s = \frac{-i}{\sqrt{2}}$. equation (3.3.36) becomes

$$\begin{aligned}|\psi_{\rm out}\rangle &= \frac{1}{\sqrt{n!}}(ca_1^\dagger + sa_2^\dagger)^n(sa_1^\dagger + ca_2^\dagger)|0.0\rangle \\ &= \frac{1}{\sqrt{n!}}\sum_{l=0}^{n}\frac{n!c^l s^{n-k+1}}{l!(n-l)!}(a_1^\dagger)^{l+1}(a_2^\dagger)^{n-l}|0.0\rangle \\ &\quad + \frac{1}{\sqrt{n!}}\sum_{l=0}^{n}\frac{n!c^{l+1}s^{n-k}}{l!(n-l)!}(a_1^\dagger)^{l}(a_2^\dagger)^{n-l+1}|0.0\rangle \\ &= \frac{1}{\sqrt{n!}}\sum_{l=0}^{n}\frac{n!(k+1)!}{\sqrt{(k+1)!(n-k)!}}c^k s^{n-k+1}|k+1.n-k\rangle \\ &\quad + \frac{1}{\sqrt{n!}}\sum_{l=0}^{n}\frac{n!(n-k+1)!}{\sqrt{(k)!(n-k+1)!}}c^{k+1}s^{n-k}|k.n-k+1\rangle. \end{aligned} \tag{3.3.37}$$

For the amplitude of the phase distribution, we have

$$\begin{aligned}\langle\theta_1,\theta_2|\psi_{\rm out}\rangle &= e^{-i(\theta_1+n\theta_2)}\sum_{l=0}^{n}\frac{\sqrt{n!}(l+1)}{\sqrt{(l+1)!(n-l)!}}c^l s^{n-l+1}e^{-i\theta_d l} \\ &\quad + e^{-i(n+1)\theta_2}\sum_{l=0}^{n}\frac{\sqrt{n!}(n-l+1)}{\sqrt{(l)!(n-l+1)!}}c^{l+1}s^{n-l}e^{-i\theta_d l}. \end{aligned} \tag{3.3.38}$$

As in the previous section, we have approximated the the factorials and changed

the summations to integrals. For the first term in the equation (3.3.38), we have

$$\begin{aligned}\langle\theta_1,\theta_2|\psi_{\text{out}}\rangle &= \frac{\sqrt{\pi n!}}{(\frac{n+1}{n})!}(\frac{1}{\sqrt{2}})^{1/2}e^{-\frac{n+1}{4}\theta_d^2}(1-i\theta_d)\{ \\ &\quad e^{-i\frac{\pi(n+1)}{2}}e^{-i(\theta_1+n\theta_2)}e^{-i\frac{\theta_d(n-1)}{2}} \\ &\quad + e^{-i\frac{\pi n}{2}}e^{-i(n+1)\theta_2}e^{-i\frac{\theta_d(n-1)}{2}}\} \qquad (3.3.39)\end{aligned}$$

From the above equation we obtain the difference phase distribution

$$P(\theta_1,\theta_2) = \frac{en^n}{(n+1)^{n+1}}\sqrt{\frac{n}{8\pi}}(1+(\theta_d-\frac{\pi}{2})^2)(1+\cos(2\theta_d))e^{-\frac{n+1}{2}(\theta_d-\frac{\pi}{2})^2}. \quad (3.3.40)$$

The width for each of the two peaks is $\frac{1}{\sqrt{n+1}}$ and this is narrower than the case for vaccum state in one of the input beam. However, the sensitivity is worse than the case of the vaccum state in one of the input beam because of the two peak structure. In order to estimate the locations of two peaks, we differentiated the equation (3.3.40) and set it equal to be zero .

$$\begin{aligned}2(\theta_d-\frac{\pi}{2})(1+\cos(2\theta_d)) &= (1+(\theta_d-\frac{\pi}{2})^2)\{ \\ &\quad (1+n)(\theta_d-\frac{\pi}{2})(1+\cos(2\theta_d)+2\sin(2\theta_d)\}. \qquad (3.3.41)\end{aligned}$$

Equation (3.3.41) is a transcedental equation and using numerical method we have identified the location of the two peaks for the case of $n = 10$, $n = 50$ and $n = 100$. For the case $n = 10$, the two peaks occur at 65.3 degrees and 114.7 degrees respectively. For the case of $n = 50$, the two peaks occur at 78.6 degrees and 101.4 degrees respectively. For the case of $n = 100$, the two peaks occur at 81.8 degrees and 98.2 degrees respectively. As the number of photons increases

, the separation of the two peaks gets smaller and smaller as expected. As we increase the number of photons in one of the input ports from one photon, the number of peaks in the difference phase distribution also increase.

For the the case of a two-photon and eight-photon input . we have three peaks; one of the peaks is smaller than the other two while the other two peaks are sharper than in the case of the $|n, 0\rangle$ state. The suppressed peak is located at $\frac{\pi}{2}$ and other sharper two peaks are located symmetrically about $\frac{\pi}{2}$. From our numerical studies we see that the number of peaks in the difference phase distribution is $n + 1$ where n is the smaller number of photons coming into one of the legs. If the n is even, then one of the peaks located at $\frac{\pi}{2}$. While the number of peaks increases as the photon number difference between the input beams decreases, these peaks will be suppressed except for the two peaks, which are the left-most and right-most. Increasing the number of photons until the photon number difference is zero, we have the two number state input with equal intensities, where two peaks occur at 0 and $\frac{\pi}{2}$. Actually, there are n+1 peaks but only two peaks matter because all the peaks between the two peaks located at 0 and $\frac{\pi}{2}$ are suppressed , so it appears that there are only two peaks for the number state inputs with equal intensities. These results are shown in Fig. (17).

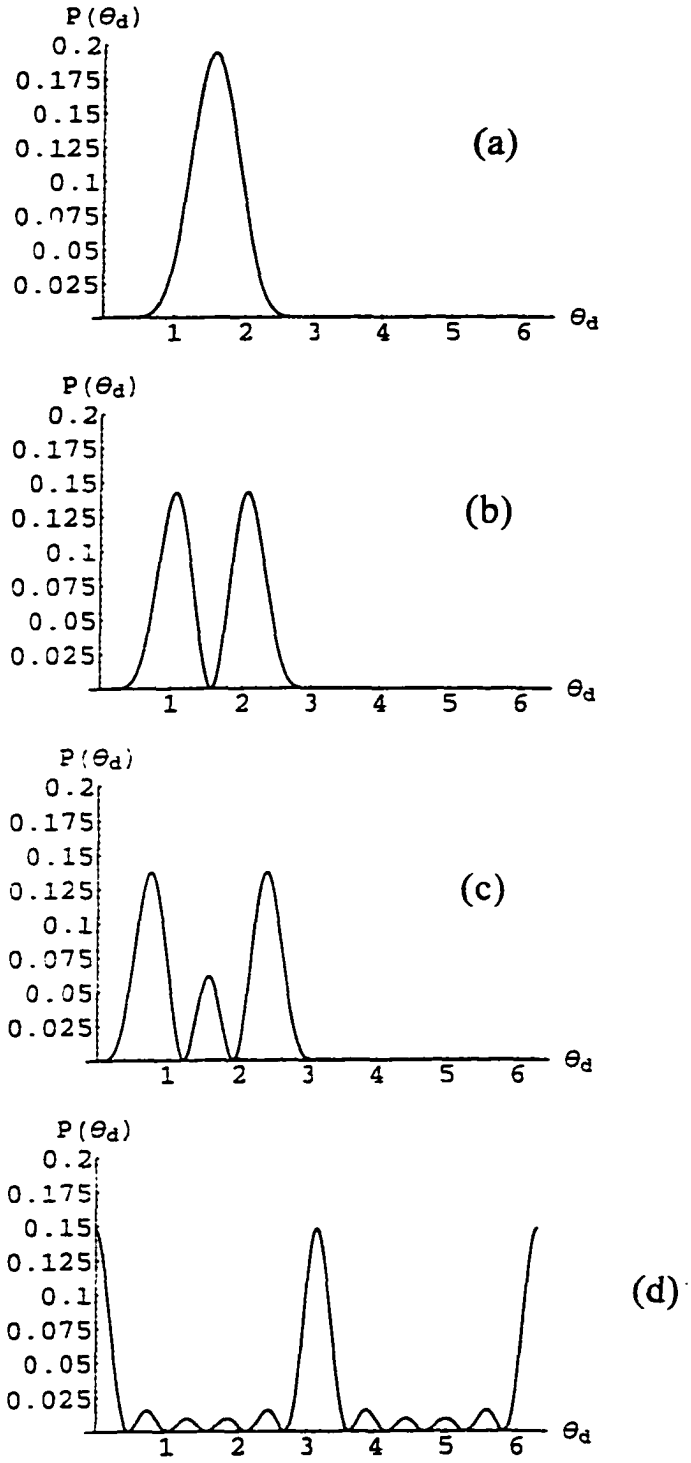

Figure 17: The difference phase distribution for a) $|10,0\rangle$ input state. b) $|9,1\rangle$ input state c) $|8,2\rangle$ input state and $|5,5\rangle$ input state

Chapter IV

4 A linear combination of number state as an input state

4.1 A state with phase

So far the number state inputs we have considered have precise number of photons and therefore. arbitrary phase due to the Heisengberg's uncertainty principle. Here we would like to consider a state with a linear combination of number states as our input state. Since the input state has an uncertainty in its photon number. the phase of the input state is no longer totally arbitrary. The state we shall send into one of the input ports of the interferometer is

$$|\upsilon\rangle = \frac{1}{(1+|v|)^2}(|n\rangle + v|n+1\rangle) \quad 0 \leq v \leq \frac{1}{\sqrt{2}}. \tag{4.1.1}$$

Then the total input state of the system becomes

$$|\upsilon_{\text{in}}\rangle = \frac{1}{(1+|v|)}(|n,n\rangle + v(|n,n+1\rangle + |n+1,n\rangle) + v^2|n+1,n+1\rangle). \tag{4.1.2}$$

The phase distribution of this input state is

$$\begin{aligned} P(\theta_1,\theta_2) &= \frac{1}{4\pi^2}|\langle\psi|\theta_1,\theta_2\rangle|^2 \\ &= (\frac{1}{4\pi^2})(\frac{1}{(1+|v|^2)^2})(1+v(\cos\theta_1+\cos\theta_2) \end{aligned}$$

$$+v^2(2+\cos(\theta_1+\theta_2)+\cos(\theta_1-\theta_2)$$

$$+v^3(\cos\theta_1+\cos\theta_2)+v^4). \qquad (4.1.3)$$

Here, we are interested in the difference phase distribution $P(\theta_d)$. However, the equation (4.1.3) has not only the term containing θ_d which we define it to be $\theta_1-\theta_2$ but also has the term containing θ_s which is defined to be $\frac{\theta_1+\theta_2}{2}$. Substituting θ_d and θ_s for θ_1 and θ_2, we have

$$\begin{aligned} P(\theta_d,\theta_s) &= (\frac{1}{4\pi^2})(\frac{1}{(1+|v|^2)^2})(1+v(2\cos\theta_s\cos\frac{\theta_d}{2}) \\ &\quad +v^2(2+\cos 2\theta_s+\cos\theta_d) \\ &\quad +v^3(2\cos\theta_s\cos\frac{\theta_d}{2})+v^4). \end{aligned} \qquad (4.1.4)$$

We need to integrate out θ_s in the phase distribution. If we integrate the phase distribution over θ_1 and θ_2, we are integrating over a square in the Cartesian coordinates whose axes are θ_1 and θ_2. With the change of integration variables, $\theta_1=\theta_s+\frac{1}{2}\theta_d, \theta_2=\theta_s-\frac{1}{2}\theta_d$, the integration over the same rectangle becomes

$$\int_0^{2\pi}d\theta_1\int_0^{2\pi}d\theta_2 P(\theta_1,\theta_2)\Rightarrow(\int_{-2\pi}^{0}d\theta_d\int_{-\frac{\theta_d}{2}}^{2\pi+\frac{\theta_d}{2}}d\theta_s+\int_0^{2\pi}d\theta_d\int_{\frac{\theta_d}{2}}^{2\pi-\frac{\theta_d}{2}}d\theta_s)P(\theta_d,\theta_s) \qquad (4.1.5)$$

After integrating out θ_s, we have difference phase distribution for $-2\pi\le\theta_d<0$

$$\begin{aligned} P(\theta_d) &= (\frac{1}{4\pi^2(1+|v|^2)^2})\{2\pi-\theta_d \\ &\quad -v(2\sin\theta_d)+v^2(4\pi-2\theta_d-\sin\theta_d+\cos\theta_d) \\ &\quad -v^3(2\sin\theta_d)+v^4(2\pi-\theta_d)\}. \end{aligned} \qquad (4.1.6)$$

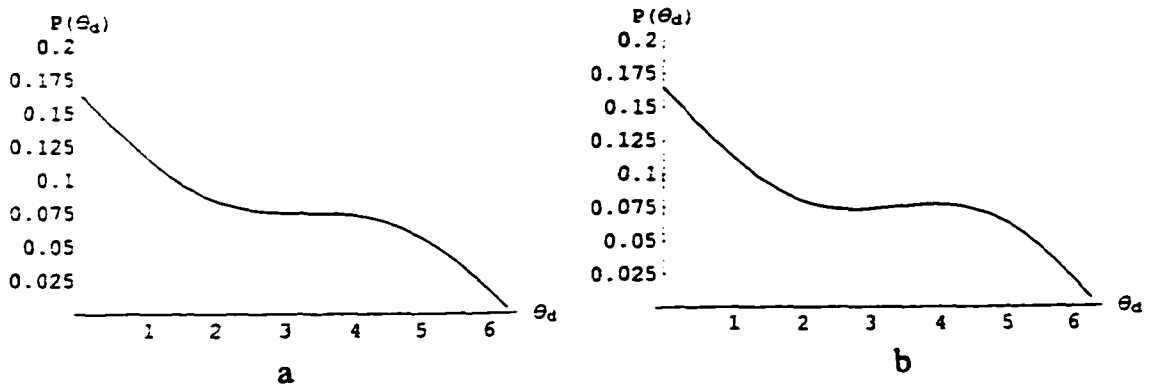

Figure 18: The difference phase distibution for the linear combinatin input state for two different values of v; a) $v = \frac{1}{2}$ case b) $v = \frac{1}{\sqrt{2}}$ case.

Also. for $0 \leq \theta_d < 2\pi$, we have

$$\begin{aligned} P(\theta_d) &= (\frac{1}{4\pi^2(1+|v|^2)^2})\{2\pi + \theta_d \\ &\quad + v(2\sin\theta_d) + v^2(4\pi + 2\theta_d + \sin\theta_d + \cos\theta_d) \\ &\quad + v^3(2\sin\theta_d) + v^4(2\pi + \theta_d)\}. \end{aligned} \tag{4.1.7}$$

From the equation (4.1.6) and (4.1.7), we know that the input state system has a phase as long as v is not zero. If v is zero, then this corresponds to the input system of two number state input with equal intensities and therefore the phase is arbitrary. In Fig. (18), we have plotted the difference phase distribution for this input state of the system for two different values of v. For nonzero v values, we expect the difference phase distribution after the beam splitter inside the interferometer will be different from the case for the number state input with equal intensities, but not too drastically different.

We have for the phase distribution of this input after the first beam splitter

$$P(\theta_1,\theta_2) = \frac{1}{2\pi(1+|v|^2)^2}\{\ |\langle\theta_1,\theta_2|n,n\rangle|^2$$
$$+ v\,(\langle\theta_1,\theta_2|n,n\rangle\langle\theta_1,\theta_2|n,n+1\rangle^* + \langle\theta_1,\theta_2|n,n\rangle\langle\theta_1,\theta_2|n+1,n\rangle^*$$
$$+ \langle\theta_1,\theta_2|n,n+1\rangle\langle\theta_1,\theta_2|n,n\rangle^* + \langle\theta_1,\theta_2|n+1,n\rangle\langle\theta_1,\theta_2|n,n\rangle^*)$$
$$+ v^2\,(\langle\theta_1,\theta_2|n,n\rangle\langle\theta_1,\theta_2|n+1,n+1\rangle^* + \langle\theta_1,\theta_2|n+1,n+1\rangle\langle\theta_1,\theta_2|n,n\rangle^*$$
$$+ |\langle\theta_1,\theta_2|n,n+1\rangle|^2 + |\langle\theta_1,\theta_2|n+1,n\rangle|^2$$
$$+ \langle\theta_1,\theta_2|n,n+1\rangle\langle\theta_1,\theta_2|n+1,n\rangle^* + \langle\theta_1,\theta_2|n+1,n\rangle\langle\theta_1,\theta_2|n,n+1\rangle^*)$$
$$+ v^3\,(\langle\theta_1,\theta_2|n,n+1\rangle\langle\theta_1,\theta_2|n+1,n+1\rangle^* + \langle\theta_1,\theta_2|n+1,n\rangle\langle\theta_1,\theta_2|n+1,n+1\rangle^*$$
$$+ \langle\theta_1,\theta_2|n+1,n+1\rangle\langle\theta_1,\theta_2|n,n+1\rangle^* + \langle\theta_1,\theta_2|n+1,n+1\rangle\langle\theta_1,\theta_2|n+1,n\rangle^*)$$
$$+ v^4|\langle\theta_1,\theta_2|n+1,n+1\rangle|^2\ \} \qquad (4.1.8)$$

For the general number of photons, we have

$$\langle\theta_1,\theta_2|U_1|n,m\rangle = \sum_{p=0}^{n}\sum_{q=0}^{m}\left(\frac{n!m!c^{p-q}s^{n+m-p-q}}{p!q!(n-p)!(m-q)!}\right.$$
$$\left.\sqrt{\frac{(m+p-q)!(n+q-p)!}{n!m!}}e^{-i(m+p-q)\theta_1+(n+q-p)\theta_2}\right) \qquad (4.1.9)$$

where $c = \frac{1}{\sqrt{2}}$ and $s = \frac{-i}{\sqrt{2}}$. By substituting the above equation into the equation (4.1.8), the difference phase distribution of this system after the first beam splitter has been computer-simulated and it is shown in Fig. (19). In Fig. (19), there is one big peak located at $\theta_d = 0$ and there is a peak at $\theta_d = \pi$. There is no peak at $\theta_d = 2\pi$. Comparing these peak structure to the case for the number state input , $|n,n\rangle$, which has same peaks at those locations, we notice that the peak

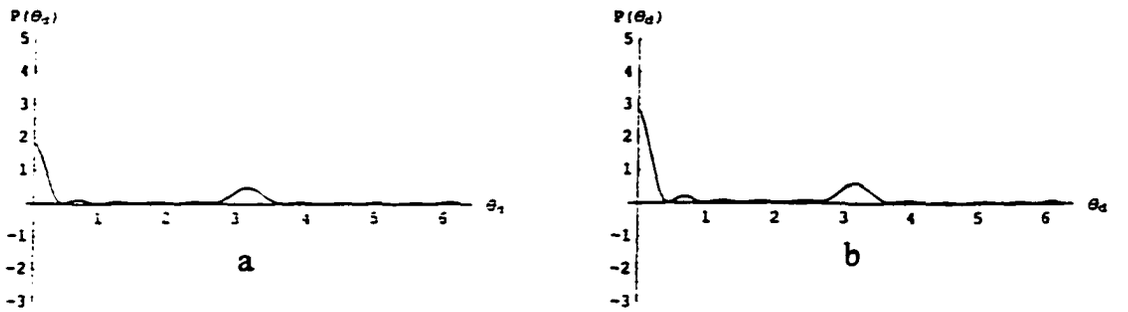

Figure 19: The difference phase distibution after the first B.S. for the linear combinatin input state for two different values of v; a) $v = \frac{1}{2}$ case b) $v = \frac{1}{\sqrt{2}}$ case.

at $\theta_d = 0$ is amplified and the peak at $\theta_d = \pi$ become smaller and there is no peak at all at $\theta_d = 2\pi$. This peak structure in the difference phase distribution allows us to utilize the narrow rotaional width of the peak which is in the order of $\frac{1}{n}$. In the two photon number state input case, $|n, n\rangle$, the peaks at $\theta_d = 0, \pi$ and 2π have the same height. This causes signal to vanish and therefore destroys the sensitivity of the interferometer. The problem of the number state input with two equal intensities is the problem of two peaks located at 0 and π with equal distribution and these two peaks contribute to cancel each other. For the input state with the linear combination of number states, peaks at $\theta_d = 0$ and π are different: the difference phase distribution around the peak at the $\theta_d = 0$ is greater than the distribution around the peak at $\theta_d = \pi$ as shown in Fig. (19). The area under the curve located around $\theta_d = 0$ is about twice as large a that

under the curve located at $\theta_d = \frac{\pi}{2}$. Thus, the contribution to the signal from these two peaks will not cancel out and therefore, we can use this signal to detect a phase shift inside a inteferometer. Using this liner combination of number state, we improve the sensitivity of the interferometer.

For this state, we have calculated the expectation value of J_3 at the output, $\langle J_{3\text{out}} \rangle$ and $\Delta J_{3\text{out}}$

$$\langle \psi | J_3 | \psi \rangle = \frac{1}{(1+|v|^2)^2}(v^2(2(n+1)\sin\phi)) \tag{4.1.10}$$

$$\langle \psi | J_3^2 | \psi \rangle = \frac{1}{(1+|v|^2)^2}(2v^2\cos^2\phi + (2n+2n^2+v^2(2+8n+4n^2) + v^4(4+6n+2n^2))\sin^2\phi). \tag{4.1.11}$$

The minimum detectable phase shift about $\phi = 0$, the sensitivity of the interferometer, is calulated to be in the order of n

$$\delta\phi = \frac{\sqrt{2}(1+|v|^2)}{v(2(n+1))} \qquad 0 \le v \le \frac{1}{\sqrt{2}}. \tag{4.1.12}$$

We can find that in equation (4.1.12) the sensitivity of the interferometer deteriorates as v approaches to zero; this is the case of the two number state input with the equal intensities. Thus, the minimum detectable phase shift in equation (4.1.12) does match in the limiting case. For $v = \frac{1}{\sqrt{2}}$, the minimum detectable phase shift is

$$\delta\phi = \frac{3}{2(n+1)}. \tag{4.1.13}$$

The minimun detectable phase shift is in the order of n and the sensitivity of the interferometer depends on the difference phase distribution after the first beam

splitter inside the interferometer; the sensitivity is directly proportional to the rotational width of the peak in the difference phase distribution. The narrower the width, the better the sensitivity. However, as shown in the number state input case with the equal intensities, if the difference phase distribution is symmetric with respect to $\theta_d = \frac{\pi}{2}$, we can not take the advantage of narrower rotational width. Now for the case of linear combination of the number state, we have good sensitivity because there is only one big peak in the difference phase distribution after the first beam splitter inside the interferometer.

4.2 Quasi-Analytic approximation for the linear combination of number states

In order to evaluate the difference phase distribtion for the large numbers of photons, we need to approximate the equation (4.1.8). We notice the equation (4.1.8) basically consists of combinations of three terms and their complex conjugates; $\langle\theta_1, \theta_2|U_1|n, n\rangle$, $\langle\theta_1, \theta_2|U_1|n+1, n\rangle$ and $\langle\theta_1, \theta_2|U_1|n, n+1\rangle$. First, we wish to approximate $\langle\theta_1, \theta_2|U_1|n, n\rangle$.

$$\begin{aligned} |\psi_{\text{out}}\rangle &= U_1|\psi_{\text{in}}\rangle = U_1|n, n\rangle \\ &= |\psi_0\rangle + |\psi_\pi\rangle \end{aligned} \tag{4.2.1}$$

where we have

$$|\psi_0\rangle = \frac{1}{2}\cos(\frac{\pi j}{2})\sum_{m=-j}^{m=j} c_m|j,m\rangle, c_m \approx \sqrt{\frac{2}{\pi}}(\frac{1}{j^2-m^2})^{\frac{1}{4}} \text{ for } m \neq j \quad (4.2.2)$$

$$|\psi_\pi\rangle = \frac{1}{2}\cos(\frac{\pi j}{2})\sum_{m=-j}^{m=j} c_m(-1)^m|j,m\rangle. \quad (4.2.3)$$

For the phase state, we have

$$\begin{aligned}|\theta_1,\theta_2\rangle &= \frac{1}{2\pi}\sum_{n_1=0}^{\infty}\sum_{n_2=0}^{\infty} e^{i(n_1\theta_1+n_2\theta_2)}|n_1,n_2\rangle \\ &= \frac{1}{2\pi}\sum_{j=0}^{\infty} e^{ij(\theta_1+\theta_2)}\sum_{m=-j}^{m=j} e^{im(\theta_1-\theta_2)} \quad (4.2.4)\end{aligned}$$

where we have used $j = \frac{1}{2}(n_1+n_2)$ and $m = \frac{1}{2}(n_1-n_2)$. Therefore, we have

$$\langle\theta_1,\theta_2|\psi_0\rangle = \frac{1}{4\pi}e^{-ij(\theta_1+\theta_2)}\cos\frac{\pi j}{2}\sum_{m=-j}^{m=j} e^{-im(\theta_1-\theta_2)}c_m. \quad (4.2.5)$$

We can approximate the above equation by changing the sum into an integral

$$\sum_{m=-j}^{m=j} e^{-im(\theta_1-\theta_2)}c_m \Rightarrow \int_{-j}^{j} dm e^{-im\phi}\frac{1}{(j^2-m^2)^{\frac{1}{4}}} \quad (4.2.6)$$

which will be good approximation for $\phi \ll 1$. By letting $x = \frac{m}{j}$, the integral in the equation (4.2.6) becomes

$$\begin{aligned}\int_{-j}^{j} e^{-im\phi}\frac{1}{(j^2-m^2)^{\frac{1}{4}}} &= \sqrt{j}\int_{-1}^{1} dx e^{-ijx\phi}\frac{1}{(1-x^2)^{\frac{1}{4}}} \\ &= \sqrt{\pi j}(\frac{2}{-j\phi})^{\frac{1}{4}}\Gamma(\frac{3}{4})J_{\frac{1}{4}}(-j\phi) \quad (4.2.7) \\ &= \sqrt{\pi j}(\frac{2}{j|\phi|})^{\frac{1}{4}}\Gamma(\frac{3}{4})J_{\frac{1}{4}}(-j|\phi|) \quad (4.2.8)\end{aligned}$$

The imaginary part of the equation (4.2.7) is an odd function and only the real part survives integration. Therefore, we can replace ϕ by $|\phi|$. The equation

(4.2.5) becomes

$$\langle\theta_1,\theta_2|\psi_0\rangle = \frac{\sqrt{2j}}{4\pi}\cos\frac{\pi j}{2}e^{-ij(\theta_1+\theta_2)}\Gamma(\frac{3}{4})(\frac{2}{j|\phi|})^{\frac{1}{4}}J_{\frac{1}{4}}(j|\phi|) \qquad (4.2.9)$$

Similarly we have

$$\langle\theta_1,\theta_2|\psi_\pi\rangle = \frac{\sqrt{2j}}{4\pi}\cos\frac{\pi j}{2}e^{-ij(\theta_1+\theta_2)}\Gamma(\frac{3}{4})(\frac{2}{j|\phi-\pi|})^{\frac{1}{4}}J_{\frac{1}{4}}(j|\phi-\pi|) \qquad (4.2.10)$$

Putting the equation(4.2.9) and (4.2.10) together, we have

$$\begin{aligned}&\langle\theta_1,\theta_2|U_1|n,n\rangle\\ &= \Big(\frac{\sqrt{2j}}{4\pi}\cos\frac{\pi j}{2}e^{ij(\theta_1+\theta_2)}\Gamma(\frac{3}{4})\\ &\{(\frac{2}{j|\phi|})^{\frac{1}{4}}J_{\frac{1}{4}}(j|\phi|)+(\frac{2}{j|\phi-\pi|})^{\frac{1}{4}}J_{\frac{1}{4}}(j|\phi-\pi|)\}\Big)\end{aligned} \qquad (4.2.11)$$

Let's consider $|\psi_{\rm in}\rangle = |n+1,n\rangle = \frac{a_1^\dagger}{\sqrt{n+1}}|n,n\rangle$. For the output state after the first beam splitter we have

$$\begin{aligned}|\psi_{\rm out}\rangle &= U_1|\psi_{\rm in}\rangle = U_1|n,n+1\rangle\\ &= U_1(\frac{a_1^\dagger}{\sqrt{n+1}})|n,n\rangle\\ &= \frac{1}{\sqrt{n+1}}U_1a_1^\dagger U_1^\dagger U_1|n,n\rangle\\ &= \frac{1}{\sqrt{n+1}}\frac{1}{\sqrt{2}}(a_1^\dagger - ia_2^\dagger)U_1|n,n\rangle\\ &= \frac{1}{\sqrt{2(n+1)}}(a_1^\dagger - ia_2^\dagger)(|\psi_0\rangle+|\psi_\pi\rangle).\end{aligned} \qquad (4.2.12)$$

We need to know how $a_1^\dagger$ and $a_2^\dagger$ operate on the the state $|j,m\rangle$. We know how the the creation and the annihilation operators act on the number state

$$\begin{aligned}a_1^\dagger|n_1,n_2\rangle &= \sqrt{n_1+1}|n_1+1,n_2\rangle\\ a_2^\dagger|n_1,n_2\rangle &= \sqrt{n_2+1}|n_1,n_2+1\rangle.\end{aligned} \qquad (4.2.13)$$

From the equation (4.2.13) and j and m, $j = \frac{1}{2}(n_1 + n_2)$ and $m = \frac{1}{2}(n_1 - n_2)$, we obtain

$$\begin{aligned} a_1^\dagger|j,m\rangle &= \sqrt{j+m+1}\,|j+\frac{1}{2},m+\frac{1}{2}\rangle \\ a_2^\dagger|j,m\rangle &= \sqrt{j-m+1}\,|j+\frac{1}{2},m-\frac{1}{2}\rangle. \end{aligned} \tag{4.2.14}$$

Using the equations (4.2.14), we have for $|\psi_{\text{out}}\rangle$

$$\begin{aligned} |\psi_{\text{out}}\rangle &= U_1|\psi_{\text{in}}\rangle \\ &= U_1|n+1,n\rangle \\ &= \frac{1}{2\sqrt{2(j+1)}}\cos(\frac{\pi j}{2})\{\sum_{m=-j}^{m=j} c_m\sqrt{j+m+1}|j+\frac{1}{2},m+\frac{1}{2}\rangle \\ &\quad + \sum_{m=-j}^{m=j} c_m(-1)^m\sqrt{j+m+1}|j+\frac{1}{2},m+\frac{1}{2}\rangle \\ &\quad - i\sum_{m=-j}^{m=j} c_m(-1)^m\sqrt{j-m+1}|j+\frac{1}{2},m-\frac{1}{2}\rangle \\ &\quad - i\sum_{m=-j}^{m=j} c_m(-1)^m\sqrt{j-m+1}|j+\frac{1}{2},m-\frac{1}{2}\rangle\} \end{aligned} \tag{4.2.15}$$

If we project the $|\psi_{\text{out}}\rangle$ onto the phase state, we have

$$\begin{aligned} \langle\theta_1,\theta_2|\psi_{\text{out}}\rangle &= \langle\theta_1,\theta_2|U_1|\psi_{\text{in}}\rangle \\ &= \langle\theta_1,\theta_2|U_1|n+1,n\rangle \\ &= \frac{1}{4\pi\sqrt{2(j+1)}}\cos(\frac{\pi j}{2})e^{-i(j+\frac{1}{2})(\theta_1-\theta_2)}\{ \\ &\quad \sum_{m=-j}^{m=j} c_m e^{-i(m+\frac{1}{2})(\theta_1-\theta_2)}\sqrt{j+m+1} \\ &\quad + \sum_{m=-j}^{m=j} c_m(-1)^m e^{-i(m+\frac{1}{2})(\theta_1-\theta_2)}\sqrt{j+m+1} \end{aligned}$$

$$-i\sum_{m=-j}^{m=j} c_m e^{-i(m-\frac{1}{2})(\theta_1-\theta_2)}\sqrt{j-m+1}$$
$$-i\sum_{m=-j}^{m=j} c_m(-1)^m e^{-i(m-\frac{1}{2})(\theta_1-\theta_2)}\sqrt{j-m+1}\}. \quad (4.2.16)$$

We want to approximate the equation (4.2.16) by turning the sums into integrals.

For the first term. we have

$$\begin{aligned}\sum_{m=-j}^{m=j} e^{-im(\theta_1-\theta_2)}c_m\sqrt{j+m+1} &\approx \sqrt{\frac{2}{\pi}}\int_{-j}^{j} dm\, e^{-im\phi}\frac{\sqrt{j+m+1}}{(j^2-m^2)^{\frac{1}{4}}} \quad \phi=\theta_1-\theta_2\\ &\approx \sqrt{\frac{2}{\pi}}\int_{-j}^{j} dm\, e^{-im\phi}(\frac{j+m}{j-m})^{\frac{1}{4}} \quad ,x=\frac{m}{j}\\ &= (j)\sqrt{\frac{2}{\pi}}\int_{-1}^{1} dx\, e^{-ijx\phi}(\frac{1+x}{1-x})^{\frac{1}{4}}. \quad (4.2.17)\end{aligned}$$

The integral in (4.2.17) can be expressed in terms of a Kummer function [23].

$$M(a,b,z)=\frac{\Gamma(b)}{\Gamma(a)\Gamma(b-a)}2^{1-b}e^{\frac{1}{2}z}\int_{-1}^{1}(1-t)^{b-a-1}(1+t)^{a-1}e^{\frac{1}{2}zt}dt. \quad (4.2.18)$$

Comparing the equation (4.2.17) and (4.2.18). we find that in our case we have $z=-2ij\phi, a=\frac{5}{4}$ and $b=2$ and the first term in the equation (4.2.16) becomes

$$\sum_{m=-j}^{m=j} c_m e^{-im\phi}\sqrt{j+m+1}\approx(2j)\,(\frac{2}{\pi})^{\frac{1}{2}}\frac{\Gamma(\frac{3}{4})\Gamma(\frac{5}{4})}{\Gamma(2)}e^{ij\phi}M(\frac{5}{4},2,-2ij\phi). \quad (4.2.19)$$

Similarly for the second term which is different from the first term by $e^{i\pi\phi}$. we have

$$\sum_{m=-j}^{m=j} c_m e^{-im(\phi-\pi)}\sqrt{j+m+1}\approx(2j)\,(\frac{2}{\pi})^{\frac{1}{2}}\frac{\Gamma(\frac{3}{4})\Gamma(\frac{5}{4})}{\Gamma(2)}e^{ij(\phi-\pi)}M(\frac{5}{4},2,-2ij(\phi-\pi)). \quad (4.2.20)$$

Combining the equations (4.2.19) and (4.2.20) we have

$$\langle\theta_1,\theta_2|a_1^{\dagger}|\{|\psi_0\rangle+|\psi_\pi\rangle\} = (\frac{j}{2\pi})\frac{e^{-i\frac{1}{2}\phi}e^{-i(j+\frac{1}{2})(\theta_1+\theta_2)}}{\sqrt{\pi(j+1)}}\cos(\frac{\pi j}{2})\frac{\Gamma(\frac{3}{4})\Gamma(\frac{5}{4})}{\Gamma(2)}$$

$$\{e^{ij\phi}M(\frac{5}{4},2,-2ij\phi)$$
$$+e^{ij(\phi-\pi)}M(\frac{5}{4},2,-2ij(\phi-\pi))\}. \qquad (4.2.21)$$

For the third term in the equation we have

$$\begin{aligned}\sum_{m=-j}^{m=j} c_m e^{-im\phi}\sqrt{j-m+1} &\approx \sqrt{\frac{2}{\pi}}\int_{-j}^{j} e^{-im\phi}\frac{1}{(j^2-m^2)^{\frac{1}{4}}}\sqrt{j-m}\,dm \\ &\approx \sqrt{\frac{2}{\pi}}\int_{-j}^{j} e^{-im\phi}(\frac{j-m}{j+m})^{\frac{1}{4}}\,dm \;x=\frac{m}{j} \\ &= (j)\sqrt{\frac{2}{\pi}}\int_{-j}^{j} e^{-ixj\phi}(1-x)^{\frac{1}{4}}(1+x)^{-\frac{1}{4}} \qquad (4.2.22)\end{aligned}$$

Comparing to the equation (4.2.18), the equation (4.2.22) becomes

$$\sum_{m=-j}^{m=j} c_m e^{-im\phi}\sqrt{j-m+1} \approx (2j)\sqrt{\frac{2}{\pi}}\frac{\Gamma(\frac{3}{4})\Gamma(\frac{5}{4})}{\Gamma(2)}e^{ij\phi}M(\frac{3}{4},2,-2ij\phi). \qquad (4.2.23)$$

Similarly for the last term which is different from the third term by $e^{i\pi\phi}$, we have

$$\sum_{m=-j}^{m=j} c_m e^{-im(\phi-\pi)}\sqrt{j-m+1} \approx (2j)\sqrt{\frac{2}{\pi}}\frac{\Gamma(\frac{3}{4})\Gamma(\frac{5}{4})}{\Gamma(2)}e^{ij(\phi-\pi)}M(\frac{3}{4},2,-2ij(\phi-\pi)). \qquad (4.2.24)$$

Combinig the equation (4.2.23) and (4.2.24), we obtain

$$\begin{aligned}\langle\theta_1,\theta_2|a_2^\dagger|\{|\psi_0\rangle+|\psi_\pi\rangle\} &= (\frac{j}{2\pi})\frac{e^{i\frac{1}{2}\phi}e^{-i(j+\frac{1}{2})(\theta_1+\theta_2)}}{\sqrt{\pi(j+1)}}\cos(\frac{\pi j}{2})\frac{\Gamma(\frac{3}{4})\Gamma(\frac{5}{4})}{\Gamma(2)} \\ &\{e^{ij\phi}M(\frac{3}{4},2,-2ij\phi) \\ &+e^{ij(\phi-\pi)}M(\frac{3}{4},2,-2ij(\phi-\pi))\}. \qquad (4.2.25)\end{aligned}$$

From the equations (4.2.21) and (4.2.25), we have

$$\langle\theta_1,\theta_2|a_1^\dagger - ia_2^\dagger|\{|\psi_0\rangle\} = (\frac{j}{2\pi})\frac{e^{ij\phi}e^{-i(j+\frac{1}{2})(\theta_1+\theta_2)}}{\sqrt{\pi(j+1)}}\cos(\frac{\pi j}{2})\frac{\Gamma(\frac{3}{4})\Gamma(\frac{5}{4})}{\Gamma(2)}$$

$$\{e^{-\frac{i}{2}\phi}M(\frac{5}{4},2,-2ij\phi)$$
$$-ie^{\frac{i}{2}\phi}M(\frac{3}{4},2,-2ij\phi)\} \qquad (4.2.26)$$

Using $M(a,b,z)=e^{z}M(b-a,b,-z)$ and $\Gamma(2)=1$, the equation (4.2.26) becomes

$$\begin{aligned}\langle\theta_1,\theta_2|(a_1^\dagger - ia_2^\dagger)|\{|\psi_0\rangle\} &= (\frac{j}{2\pi})\frac{e^{i(j+\frac{1}{2})\phi}e^{-i(j+\frac{1}{2})(\theta_1+\theta_2)}}{\sqrt{\pi(j+1)}}\cos(\frac{\pi j}{2})\Gamma(\frac{3}{4})\Gamma(\frac{5}{4})\\ &\{e^{-i(2j+1)\phi}M(\frac{3}{4},2,2ij\phi)\\ &-iM(\frac{3}{4},2,-2ij\phi)\}. \qquad (4.2.27)\end{aligned}$$

Similarly, we have

$$\begin{aligned}\langle\theta_1,\theta_2|(a_1^\dagger - ia_2^\dagger)|\{|\psi_\pi\rangle\} &= (\frac{j}{2\pi})\frac{e^{i(j+\frac{1}{2})(\phi-\pi)}e^{-i(j+\frac{1}{2})(\theta_1+\theta_2)}}{\sqrt{\pi(j+1)}}\cos(\frac{\pi j}{2})\Gamma(\frac{3}{4})\Gamma(\frac{5}{4})\\ &\{-ie^{-i(2j+1)(\phi-\pi)}M(\frac{3}{4},2,2ij(\phi-\pi))\\ &-iM(\frac{3}{4},2,-2ij(\phi-\pi))\}. \qquad (4.2.28)\end{aligned}$$

Finally, putting everything together, we have

$$\begin{aligned}\langle\theta_1,\theta_2|a_1^\dagger - ia_2^\dagger|\psi_{\text{out}}\rangle &\approx (\frac{j}{2\pi})\frac{1}{\sqrt{\pi(j+1)}}\cos(\frac{\pi j}{2})\Gamma(\frac{3}{4})\Gamma(\frac{5}{4})e^{-i(j+\frac{1}{2})(\theta_1+\theta_2)}\\ &\{e^{i(j+\frac{1}{2})\phi}\{e^{-i(2j+1)\phi}M(\frac{3}{4},2,2ij\phi)-iM(\frac{3}{4},2,-2ij\phi)\}\\ &+\{e^{i(j+\frac{1}{2})(\phi-\pi)}\{-ie^{-i(2j+1)(\phi-\pi)}M(\frac{3}{4},2,2ij(\phi-\pi))\\ &-iM(\frac{3}{4},2,-2ij(\phi-\pi))\}\}. \qquad (4.2.29)\end{aligned}$$

Similarly for the case of $|n,n+1\rangle$ input state, we have

$$\langle\theta_1,\theta_2|a_1^\dagger - ia_2^\dagger|\psi_{\text{out}}\rangle \approx (\frac{j}{2\pi})\frac{1}{\sqrt{\pi(j+1)}}\cos(\frac{\pi j}{2})\Gamma(\frac{3}{4})\Gamma(\frac{5}{4})e^{-i(j+\frac{1}{2})(\theta_1+\theta_2)}$$

$$\{e^{i(j+\frac{1}{2})\phi}\{-ie^{-i(2j+1)\phi}M(\frac{3}{4},2,2ij\phi)+M(\frac{3}{4},2,-2ij\phi)\}$$
$$+\{e^{i(j+\frac{1}{2})(\phi-\pi)}\{-e^{-i(2j+1)(\phi-\pi)}M(\frac{3}{4},2,2ij(\phi-\pi))$$
$$+iM(\frac{3}{4},2.-2ij(\phi-\pi))\}\}. \qquad (4.2.30)$$

Now we have approximated all three terms and we have done a computer simulation of the difference phase distribution based upon these approximation for the large numbers of photons. In Fig. (20). those reults are plotted and they show roughly the same difference phase distribution; one big peak at $\theta_d = 0$ and a small peak at $\theta_d = \pi$.

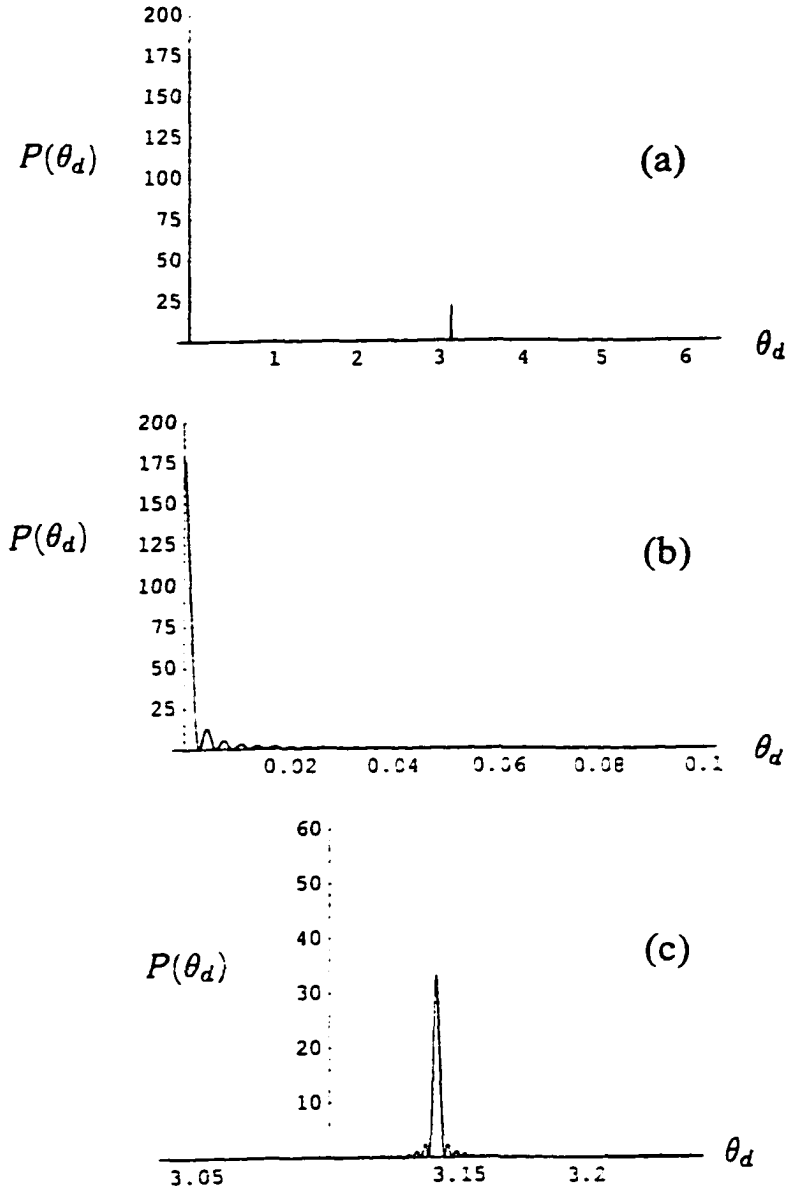

Figure 20: The difference phase distibution based upon psuedo analytic approximation for $n = 1000$ and for $v = \frac{1}{\sqrt{2}}$; a) difference phase distribution for $0 \leq \theta_d \leq 2\pi$ b) difference phase distribution around $\theta_d = 0$ c) difference phase distribution around $\theta_d = \pi$.

Chapter V

5 The effect of losses

5.1 Changes in the phase distribution due to losses

So far our discussion has been confined to the case of lossless situation. In this chapter we deal with effect of losses on the difference phase distribution. For this purpose we begin by choosing the cosine difference state to study how losses will change the difference phase distribution. Let us consider a field mode in an initial state $\rho(0)$ which is coupled to a loss reservoir. The density matrix obeys the master equation

$$\frac{d\rho}{dt} = \frac{\gamma}{2}(2a\rho a^{\dagger} - a^{\dagger}a\rho - \rho a^{\dagger}a). \tag{5.1.1}$$

We wish to evaluate the phase distribution.

$$P(\theta_1, \theta_2) = \frac{1}{4\pi^2}\langle\theta_1, \theta_2|\rho(t)|\theta_1, \theta_2\rangle. \tag{5.1.2}$$

At $t = 0$ we assume the state of the system is in cosine difference state

$$|\cos\theta_{Nr}\rangle = \frac{2}{N+2}\sum_{n=0}^{N}\sin[(n+1)\theta_{Nr}]|n, N-r\rangle \tag{5.1.3}$$

where $r = 1, 2, \ldots, N+1$. We will use the r=1 cosine difference phase state

$$|\cos\theta_{N1}\rangle = \frac{2}{N+2}\sum_{n=0}^{N}\sin[(n+1)\theta_{N1}]|n, N-1\rangle. \tag{5.1.4}$$

This state has a precise phase and its difference phase distribution has a narrow peak at $\theta_d = 0$. Using the equation (5.1.4), we would like to study how the single peak changes due to losses as time progresses. At $t = 0$, we assume the state to be in $|\cos\theta_{N1}\rangle$. Thus, we have for the field density operator at $t = 0$

$$\rho(t=0) = |\cos\theta_{N1}\rangle\langle\cos\theta_{N1}|$$
$$= \frac{2}{N+2}\sum_{n=0}^{N}\sum_{n'=0}^{N}\sin[(n+1)\theta_{N1}]\sin[(n'+1)\theta_{N1}]\rho_{n_1n_1'}(0)\rho_{n_2n_2'}(0) \quad (5.1.5)$$

where $\eta_{n_1n_1'}(0) = |n_1\rangle\langle n_1'| = |n\rangle\langle n'|$ and $\eta_{n_2n_2'}(0) = |n_2\rangle\langle n_{2'}| = |N-n\rangle\langle N-n'|$. From the above equation, we obtain the time-dependent field density matrix

$$\rho(t) = |\cos\theta_{N1}(t)\rangle\langle\cos\theta_{N1}(t)|$$
$$= \tfrac{2}{N+2}\sum_{n=0}^{N}\sum_{n'=0}^{N}\sin[(n+1)\theta_{N1}]\sin[(n'+1)\theta_{N1}]\eta(t)_{n_1n_1'}\eta(t)_{n_2n_2'} \quad (5.1.6)$$

where

$$\eta_{n_1n_1'}(t) = {}^{-\frac{\gamma t}{2}a_1^\dagger a_1}\sum_{l=0}^{\infty}\frac{(1-e^{-\gamma t})^l}{l!}(a_1)^l\eta_{n_1n_1'}(0)(a_1^\dagger)^l e^{-\frac{\gamma t}{2}a_1^\dagger a_1} \quad (5.1.7)$$

and

$$\eta_{n_2n_2'}(t) = e^{-\frac{\gamma t}{2}a_2^\dagger a_2}\sum_{l=0}^{\infty}\frac{(1-e^{-\gamma t})^l}{l!}(a_2)^l\eta_{n_2n_2'}(0)(a_2^\dagger)^l e^{-\frac{\gamma t}{2}a_2^\dagger a_2} \quad (5.1.8)$$

come from the solution of equation (5.1.1). Using equation (5.1.6), equation (5.1.2) becomes

$$P(\theta_1,\theta_2) = \frac{1}{\pi(N+2)}$$
$$\left\{\sum_{n=0}^{N}\sum_{n'=0}^{N}\sum_{l=0}^{N}\sum_{k=0}^{N}\sin[(n+1)\theta_{N1}]\sin[(n'+1)\theta_{N1}]e^{-\gamma tN}e^{-i(n'-n)\theta_d}e^{\gamma t(l+k)}\right.$$
$$\left.\frac{(1-e^{-\gamma t})^{l+k}}{l!k!}\left(\frac{n!n'!(N-n)!(N-n'!)}{(n-l)!(n'-l)!(N-n'!-k!)(N-n-k)!}\right)^{1/2}\right\}. \quad (5.1.9)$$

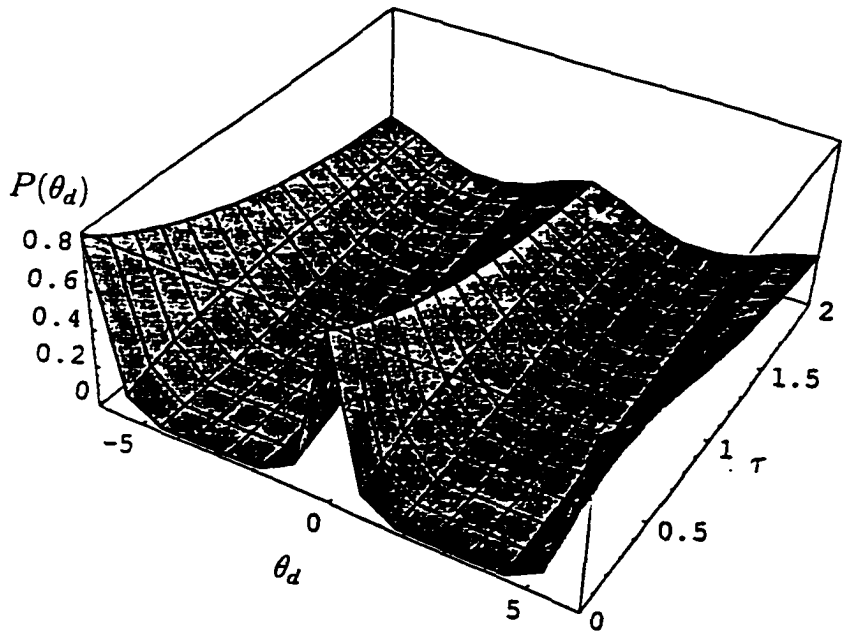

Figure 21: The changes in the phase distribution due to losses for cosine difference state.

In Fig. (21), we have plotted the above equation and find that phase distribution gets quickly broadend as time progresses due to the losses;when $\tau = \gamma t$ is 2, then the difference phase distribution flattens out. We wish to have an analytic approximation about how fast the sharp phase distribution spreads out.

We want to examine the effects of the losses on the phase of the state by finding the expectation of the operator E_- as a function of time. We define E_- to be $e^{i\phi}$, $E_- \equiv e^{i\phi}$. If $|\langle E_- \rangle|$ is close to 1, then the phase is well defined, i. e. the phase distribution has a sharp peak, but if it is significantly less than 1, then the phase distribution is broad. We expect to find that the losses cause an initially

sharp phase distribution to spread out, and the question we wish to answer is how fast this happens.

Multiplying equation (5.1.1) by E_- and taking the trace of both sides, we find that

$$\frac{d}{dt}\langle E_-\rangle = \frac{\gamma}{2}\langle(2a^\dagger E_- a - E_- a^\dagger a - a^\dagger a E_-)\rangle. \tag{5.1.10}$$

Using the fact that

$$E_- N = (N+1)E_- \qquad a = E_-\sqrt{N}, \tag{5.1.11}$$

where $N = a^\dagger a$, we find that

$$2a^\dagger E_- a - E_- N - N E_- = (2a^\dagger E_-\sqrt{N+1} - (2N+1))E_-. \tag{5.1.12}$$

Furthermore, we have that

$$2a^\dagger E_-\sqrt{N+1} - (2N+1) = 2\sqrt{N(N+1)} - (2N+1). \tag{5.1.13}$$

which gives us

$$\frac{d}{dt}\langle E_-\rangle = \gamma\langle(\sqrt{N(N+1)} - (N+\frac{1}{2}))E_-\rangle. \tag{5.1.14}$$

Applying the Schwarz inequality, we obtain an upper bound for the derivative of $\langle E_-\rangle$

$$\left|\frac{d}{dt}\langle E_-\rangle\right| \leq \gamma[\langle(\sqrt{N(N+1)} - (N+\frac{1}{2}))^2\rangle]^{1/2} \tag{5.1.15}$$

Finally, noting that

$$\begin{aligned}\sqrt{N(N+1)} - (N+\frac{1}{2}) &= \frac{N(N+1) - (N+\frac{1}{2})^2}{\sqrt{N(N+1)} + (N+\frac{1}{2})} \\ &= -\frac{1}{4(\sqrt{N(N+1)} + (N+\frac{1}{2}))}\end{aligned} \tag{5.1.16}$$

and that $\sqrt{N(N+1)} \geq N$, we find

$$\left|\frac{d}{dt}\langle E_-\rangle\right| \leq \frac{\gamma}{4}\left\langle \frac{1}{(2N+\frac{1}{2})^2}\right\rangle^{1/2}. \tag{5.1.17}$$

This inequality implies that the rate at which losses cause the phase distribution is related in a simple way to the photon number. For large photon numbers the phase spreads slowly while for small photon numbers it spread quickly. There will be some dependence on the exact form of the number distribution. In particular, for two states with the same mean photon number but different phase width, the phase of the state with the smaller phase width will diffuse more rapidly. This is because it will have a broader number distribution implying that smaller photon numbers will have a greater weight leading to a larger derivative for $\langle E_-\rangle$.

In order to proceed we need to find the time dependence of the right-hand side of Eq. (5.1.17). Taking its time derivative we find

$$\begin{aligned}\frac{d}{dt}\left\langle \frac{1}{(2N+\frac{1}{2})^2}\right\rangle &= \gamma\left\langle a^\dagger \frac{1}{(2N+\frac{1}{2})^2}a - \frac{N}{(2N+\frac{1}{2})^2}\right\rangle \\ &= \sum_{n=0}^{\infty} n\rho_{nn}\frac{8n-2}{(2n-\frac{3}{2})^2(2n+\frac{1}{2})^2}.\end{aligned} \tag{5.1.18}$$

This can be expressed as

$$\frac{d}{dt}\left\langle \frac{1}{(2N+\frac{1}{2})^2}\right\rangle = 2\gamma\sum_{n=0}^{\infty}\rho_{nn}g(n)\frac{1}{(2n+\frac{1}{2})^2}. \tag{5.1.19}$$

where

$$g(n) = \frac{2n(2n-\frac{1}{2})}{(2n-\frac{3}{2})^2}$$

$$= 1 + \frac{5}{2(2n-\frac{3}{2})} + \frac{3}{2(2n-\frac{3}{2})^2}. \qquad (5.1.20)$$

The function $g(n)$ takes its maximum value of 12 when $n = 1$. Making use of this fact gives us the inequality

$$\frac{d}{dt}\left\langle \frac{1}{(2N+\frac{1}{2})^2} \right\rangle = 24\gamma \left\langle \frac{1}{(2N+\frac{1}{2})^2} \right\rangle. \qquad (5.1.21)$$

The factor of 24 is really too large under most circumstances. It is a consequence of evaluating $g(n)$ at its maximum value, which implies that this factor will only be accurate if the photon number distribution is peaked near $n = 1$ where $g(n)$ reaches its maximum. If the photon number is concentrated near large photon numbers, which is the case of interest, then it should be possible to replace $g(n)$ by something close to its limiting value of 1.

In order to take these considerations into account we split the sum on the right-hand side of Eq. (5.1.19) into two parts an a particular value of n which we shall denote by n_0. Defining

$$F(t) = \left\langle \frac{1}{(2N+\frac{1}{2})^2} \right\rangle. \qquad (5.1.22)$$

we have that

$$\begin{aligned} \frac{dF}{dt} &= 2\gamma \left[\sum_{n=0}^{n_0} \rho_{nn} \frac{g(n)-g(n_0)}{(2n+\frac{1}{2})^2} + \sum_{n=0}^{n_0} \rho_{nn} \frac{g(n_0)}{(2n+\frac{1}{2})^2} + \sum_{n=n_0+1}^{\infty} \rho_{nn} \frac{g(n)}{(2n+\frac{1}{2})^2} \right] \\ &\leq 2\gamma s(n_0)\langle P_{n_0}\rangle + 2\gamma g(n_0) F, \end{aligned} \qquad (5.1.23)$$

where

$$s(n_0) = \sup \left| \frac{g(n)-g(n_0)}{(2n+\frac{1}{2})^2} \right| \quad \text{for} \quad 0 \leq n \leq n_0, \qquad (5.1.24)$$

and P_{n_0} is the projection onto the number states containing n_0 or fewer photons. i. e.

$$P_{n_0} = \sum_{n=0}^{n_0} |n\rangle\langle n|. \tag{5.1.25}$$

Making use of the fact that $F \leq 4$, which follows immediately from its definition. the inequality in Eq. (5.1.23) gives us that

$$\frac{1}{F}\frac{dF}{dt} \leq 8\gamma s(n_0)\langle P_{n_0}\rangle + 2\gamma g(n_0). \tag{5.1.26}$$

Integrating and then exponentiating both sides of this inequality yields

$$F(t) \leq F(0)\exp[2g(n_0)\gamma t + 8s(n_0)\gamma \int_0^t dt'\langle P_{n_0}(t')\rangle]. \tag{5.1.27}$$

For large initial photon number, we expect that $\langle P_{n_0}\rangle$ will be small (if n_0 is chosen to be much smaller than the mean number of photons), so that the behavior of the exponent in the above inequality will be dominated by the first term. which is approximately $2t$.

Finally, we can use the above result for $F(t)$ to find an upper bound for $\langle E_-\rangle$. We have that

$$\begin{aligned} |\langle E_-(t)\rangle - \langle E_-(0)\rangle| &\leq \int_0^t dt' \left|\frac{d}{dt'}\langle E_-(t')\rangle\right| \\ &\leq \frac{\gamma}{4}\int_0^t dt'\sqrt{F(t')}. \end{aligned} \tag{5.1.28}$$

In the event that $\langle P_{n_0}\rangle$ is small the right-hand side of the above inequality is approximately given by

$$\frac{1}{4}\sqrt{F(0)}(e^{\gamma t} - 1). \tag{5.1.29}$$

This should give a good estimate of how the phase of a state, which initially has a large number of photons, spreads.

5.2 Losses in a 2-mode system

So far we have only discussed one mode system and we like to extend discussion in (5.1) to two mode system. For a two mode system we have $A = E_{1-}E_{2+}$ and $A^+ = E_{1+}E_{2-}$ and we like to fine the expectation value of A. $\langle A \rangle$. as a fucntion of time which is two mode analog of E_- for the single mode system. For the master equation for this system, we have

$$\frac{d\rho}{dt} = \frac{\gamma}{2}(2a_1\rho a_1^\dagger - a_1^\dagger a_1\rho - \rho a_1^\dagger a_1 + 2a_2\rho a_2^\dagger - a_2^\dagger a_2\rho - \rho a_2^\dagger a_2). \tag{5.2.1}$$

Multiplying the above equation by A and taking the trace of both sides. we obtain

$$\frac{d}{dt}\langle A \rangle = \frac{\gamma}{2}\langle (2a_1^\dagger A a_1 - A a_1^\dagger a_1 - a_1^\dagger a_1 A) + (2a_2^\dagger A a_2 - A a_2^\dagger a_2 - a_2^\dagger a_2 A)\rangle. \tag{5.2.2}$$

Now let's look at the first three terms, $2a_1^\dagger A a_1 - A a_1^\dagger a_1 - a_1^\dagger a_1 A$. As in the single mode case. we have

$$2a_1^\dagger A a_1 - A a_1^\dagger a_1 - a_1^\dagger a_1 A = (2\sqrt{N_1(N_1+1)} - (2N_1+1))A \tag{5.2.3}$$

using the fact

$$AN_1 = E_{1-}E_{2+}N_1 = (N_1+1)A \tag{5.2.4}$$

and

$$a_1^\dagger A a_1 = \sqrt{N_1}E_{1+}E_{1-}E_{2+}E_{1-}\sqrt{N_1}$$

$$= \sqrt{N_1}(I - |0\rangle_{11}\langle 0|)E_{2+}E_{1-}\sqrt{N_{1-}}$$

$$= \sqrt{N_1(N_1+1)}A \tag{5.2.5}$$

where $N_1 = a_1^\dagger a_1$. Now look at $2a_2^\dagger A a_2 - A a_2^\dagger a_2 - a_2^\dagger a_2 A$. Similarly, we find

$$2a_2^\dagger A a_2 - AN_2 - N_2 A = A(2\sqrt{N_2(N_2+1)} - (2N_2+1)) \tag{5.2.6}$$

using the fact

$$N_2 A = N_2 E_{1-}E_{2+} = A(N_2+1) \tag{5.2.7}$$

and

$$\begin{aligned} a_2^\dagger A a_2 &= \sqrt{N_2}E_{2+}E_{1-}E_{2-}\sqrt{N_2} \\ &= A\sqrt{(N_2+1)}E_{2+}E_{2-}\sqrt{N_2} \\ &= A\sqrt{(N_2+1)(N_2)} \end{aligned} \tag{5.2.8}$$

where $N_2 = a_2^\dagger a_2$. Therefore, we have an upper bound for the derivative of $\langle A\rangle$ after applying the Schwarz inequality

$$\begin{aligned} \left|\frac{d}{dt}A\right| &= \frac{\gamma}{2}\left|\left\langle(2\sqrt{N_1(N_1+1)} - (2N_1+1))A\right\rangle + \left\langle A(2\sqrt{N_2(N_2+1)} - (2N_2+1))\right\rangle\right| \\ &\le \gamma\left[\left\langle(\sqrt{N_1(N_1+1)} - (N_1+\frac{1}{2}))^2\right\rangle^{1/2} + \left\langle(\sqrt{N_2(N_2+1)} - (N_2+\frac{1}{2}))^2\right\rangle^{1/2}\right] \\ &\le \frac{\gamma}{4}\left[\left\langle\frac{1}{(2N_1+\frac{1}{2})^2}\right\rangle^{1/2} + \left\langle\frac{1}{(2N_1+\frac{1}{2})^2}\right\rangle^{1/2}\right]. \end{aligned} \tag{5.2.9}$$

The equation (5.2.9) is essentially the same as the equation (5.1.15) and can be treated in the same way as before. So if we have

$$F_j(t) = \langle\frac{1}{(2N_j+\frac{1}{2})^2}\rangle \tag{5.2.10}$$

then

$$F_j(t) \leq F_j(0) \exp\left[2g(n_0)\gamma t + 8s(n_0)\gamma \int_0^t dt' \langle P_{n_0}^{(j)}(t')\rangle\right] \tag{5.2.11}$$

where

$$P_{n_0}^{(1)} = \sum_{n_1=0}^{n_0} |n_1\rangle\langle n_1| \otimes I_2 \tag{5.2.12}$$

and similarly for $P_{n_0}^{(2)}$

$$P_{n_0}^{(2)} = \sum_{n_2=0}^{n_0} |n_2\rangle\langle n_2| \otimes I_1. \tag{5.2.13}$$

Finally, putting everything together, we have

$$\begin{aligned} |\langle A(t)\rangle - \langle A(0)\rangle| &\leq \int_0^t dt' \left|\frac{d}{dt'}\langle A(t')\rangle\right| \\ &\leq \frac{\gamma}{4}\int_0^t dt' (\sqrt{F_1(t')} + \sqrt{F_2(t')}) \\ &\approx \frac{1}{4}\left[\sqrt{F_1(0)}(e^{\gamma t} - 1) + \sqrt{F_2(0)}(e^{\gamma t} - 1)\right]. \end{aligned} \tag{5.2.14}$$

5.3 Comparison of the effect of losses for two different states

In this section we would like to compare a coherent state and a state with well-defined difference phase to examine the effects of the losses on the phase of state . For a state with well-defined difference phase we take

$$|\psi\rangle = \eta \sum_{n=0}^{N-1} \sin\left(\frac{\pi n}{N}\right)|n\rangle \tag{5.3.1}$$

where η is a constant to be determined from the normalization requirement.

Then, we have

$$\begin{aligned}\langle\psi|\psi\rangle = 1 &= \eta^2 \sum_{n=0}^{N-1} \sin^2(\frac{\pi n}{N}) \\ &= \frac{1}{2}\eta^2 \sum_{n=0}^{N-1}(1-\cos(\frac{2\pi n}{N})).\end{aligned} \tag{5.3.2}$$

The summation of cosine term in the equation (5.3.37) is evaluated

$$\sum_{n=0}^{N-1}\cos(\frac{2\pi n}{N}) = Re\sum_{n=0}^{N-1} e^{\frac{2\pi i n}{N}} = Re\left(\frac{e^{\frac{2\pi i N}{N}}-1}{e^{\frac{2\pi i}{N}}-1}\right) = 0. \tag{5.3.3}$$

Using the above equation , we find

$$\begin{aligned}\langle\psi|\psi\rangle = 1 &= \eta^2 \sum_{n=0}^{N-1} \sin^2(\frac{\pi n}{N}) \\ &= \frac{1}{2}\eta^2 \sum_{n=0}^{N-1}(1-\cos(\frac{2\pi n}{N})) \\ &= \frac{1}{2}\eta^2 N\end{aligned} \tag{5.3.4}$$

so that the normalization constant is $\eta = \sqrt{\frac{2}{N}}$. For the mean photon numbers in this state, we have

$$\langle\psi|n|\psi\rangle = \frac{2}{N}\sum_{n=0}^{N-1} n\sin^2(\frac{\pi n}{N}) = \frac{1}{N}\sum_{n=0}^{N-1} n\left(1-\cos(\frac{2\pi n}{N})\right) \tag{5.3.5}$$

In order to calculate the equation (5.3.5), we need to evalute the $n\cos(\frac{2\pi n}{N})$ term in the summation and we have

$$\sum_{n=0}^{N-1} n\cos(\frac{2\pi n}{N}) = Re\sum_{n=0}^{N-1} ne^{\frac{2\pi i n}{N}} = Re\left\{\frac{d}{d\lambda}\sum_{n=0}^{N-1} e^{\lambda n}|_{\lambda=\frac{2\pi i}{N}}\right\}. \tag{5.3.6}$$

After summing the equation (5.3.5) over n and differentiating and evaluating the expressing at $\lambda = \frac{2\pi i}{N}$, we have

$$\frac{d}{d\lambda}\frac{e^{\lambda N}-1}{e^{\lambda}-1}\Big|_{\lambda=\frac{2\pi i}{N}} = \frac{Ne^{\lambda N}(e^{\lambda}-1)-(e^{\lambda N}-1)e^{\lambda}}{(e^{\lambda}-1)^2}\Big|_{\lambda=\frac{2\pi i}{N}} = \frac{N}{e^{\frac{2\pi i}{N}}-1}. \tag{5.3.7}$$

For the real part of the equation (5.3.7), we have

$$Re\left\{\frac{N}{e^{\frac{2\pi i}{N}}-1}\right\} = Re\left\{\frac{N(e^{\frac{-2\pi in}{N}}-1)}{2(1-\cos(\frac{2\pi}{N}))}\right\} = -\frac{N}{2}. \tag{5.3.8}$$

With the above equation and the equation (5.3.6). we find the mean number of photons in this state to be

$$\langle\psi|n|\psi\rangle = \frac{1}{N}\left[\frac{N(N-1)}{2}+\frac{N}{2}\right] = \frac{N}{2}. \tag{5.3.9}$$

Similarly we have for the difference phase operator

$$\begin{aligned}\langle\psi|E_-|\psi\rangle &= \frac{2}{N}\sum_{n=0}^{N-1}\sin(\frac{\pi n}{N})\sin(\frac{\pi(n+1)}{N}) \\ &= \frac{1}{N}\sum_{n=0}^{N-1}\left[\cos(\frac{\pi}{N})-\cos(\frac{\pi(2n+1)}{N})\right]\end{aligned} \tag{5.3.10}$$

From

$$\sum_{n=0}^{N-1}\cos(\frac{\pi(2n+1)}{N}) = Re\left\{\sum_{n=0}^{N-1}e^{\frac{\pi(2n+1)i}{N}}\right\} = Re\left\{e^{i\pi}\sum_{n=0}^{N-1}e^{\frac{2n\pi i}{N}}\right\} = 0 \tag{5.3.11}$$

we obtain the expectation value for the difference phase operator

$$\langle\psi|E_-|\psi\rangle = \cos(\frac{\pi}{N}). \tag{5.3.12}$$

We have

$$1-|\langle\psi|E_-|\psi\rangle|^2 = 1-\cos^2(\frac{\pi}{2}) \simeq 1-(1-\frac{1}{2}(\frac{\pi}{N})^2)^2 = (\frac{\pi}{N})^2. \tag{5.3.13}$$

Therefore. we have for the minimum detectable phase shift for this state

$$\Delta\phi \equiv (1-|\langle\psi|E_-|\psi\rangle|^2)^{\frac{1}{2}} = \frac{\pi}{N}. \tag{5.3.14}$$

For a coherent state $|\alpha\rangle$, we have for the mean of difference phase state

$$\begin{aligned}\langle\alpha|E_-|\alpha\rangle = \frac{\alpha}{\sqrt{\overline{n}+1}}(1+\frac{3\overline{n}}{8(\overline{n}+1)^2}) &\simeq \frac{\alpha}{\sqrt{\overline{n}}}(\sqrt{\frac{\overline{n}}{\overline{n}+1}})(1+\frac{3}{8\overline{n}}) \\ &\simeq \frac{\alpha}{\sqrt{\overline{n}}}(1-\frac{1}{2\overline{n}})(1+\frac{3}{8\overline{n}}) \\ &\simeq \frac{\alpha}{\sqrt{\overline{n}}}(1-\frac{1}{4\overline{n}}) \qquad (5.3.15)\end{aligned}$$

where $\overline{n}$ is the mean number of photons in this state. For the coherent state , the minimum detectable phase shift is in the order of $1/\sqrt{n}$

$$\begin{aligned}\Delta\phi &\equiv (1-|\langle\psi|E_-|\psi\rangle|^2)^{\frac{1}{2}} \\ &\approx (1-(1-\frac{1}{4\overline{n}})^2)^{\frac{1}{2}} \\ &= \frac{1}{\sqrt{2\overline{n}}} \qquad (5.3.16)\end{aligned}$$

At $t = 0$ the state with a well-defined difference phase has a sensitivity of $1/n$ while the coherent state has a sensitivity of $1/\sqrt{n}$. Now we want to find how the upper bounds for the difference phase change for these two states as a function of mean number of photons. From the equation 5.1.17, we have

$$\left|\frac{d}{dt}\langle E_-\rangle\right| \leq \frac{\gamma}{4}\left\langle\frac{1}{(2N+\frac{1}{2})^2}\right\rangle^{1/2}.$$

For the coherent state, we obtain the expectation value of $\frac{1}{(2N+\frac{1}{2})^2}$.

$$\langle\alpha|\frac{1}{(2N+\frac{1}{2})^2}|\alpha\rangle = e^{-|\alpha|^2}\sum_{n=0}^{\infty}\frac{|\alpha|^{2n}}{n!}\left(\frac{1}{4n^2+2n+\frac{1}{4}}\right). \qquad (5.3.17)$$

and for the state with a well-defined difference phase, we have

$$\langle\psi|\frac{1}{(2N+\frac{1}{2})^2}|\psi\rangle = \frac{2}{N}\sum_{n=0}^{N-1}\sin^2(\frac{\pi n}{N})\left(\frac{1}{4n^2+2n+\frac{1}{4}}\right) \qquad (5.3.18)$$

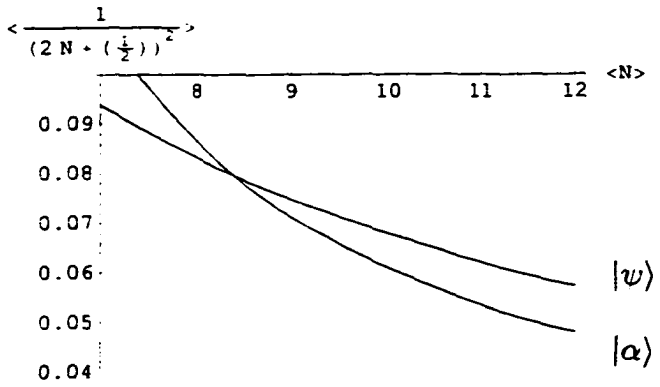

Figure 22: Plot of $\langle \frac{1}{(2N+\frac{1}{2})^2} \rangle$ as a function of the mean number of photons. $\langle N \rangle$.

In Fig. (22), we have plotted equation (5.3.17) and (5.3.18) as a function of the mean number of photons. $\langle N \rangle$. For a small number of photon numbers.one to eight photons. the coherent state has bigger upper bound in the change in the phase. For large number of photon numbers, the state with a well-defined difference phase has a bigger uppper bound and it means that the phase noise in the state with a well-defined phase is increasing faster than in the state whose phase is not as well-defined. This suggests that for large photon-numbers states with very sharply defined phases, which are intrinsically quantum mechanical. are more susceptible to the effects of losses than are classical states. such as coherent states.

Chapter VI

6 Conclusions

Applying the quantum phase formalism. we have studied the relation between the phase distribution of the quantum state inside an interferometer to the sensitivity of interferometer. Follwing the classical analysis, we have studied the effect of quantum amplitude squeezing of input beams on the sensitivity of interferometer. Classical analysis predicted that difference phase squeezing can be achieved inside the interferometer from amplitude squeezing of the input beams as long as phase fluctuations of the input beams are less than $\frac{\pi}{4}$. For this purpose we have employed squeezed states as input beams. For this squeezed state. we have studied the relation between quantum amplitude fluctuation and sensitivity of the interferometer and we found that as we squeezed the quantum amplitude fluctuations up to the point of maximum squeezing, the sensitivity of the interferometer improved. We also found that at the maximum amplitude squeezing, the phase fluctuations in the input beam were well below $\frac{\pi}{4}$. The quantum analysis confirmed the classical one; the sensitivity of the interferometer depends on the phase distribution of quantum state inside the interferometer, and the sharper the width of the peak in difference phase distribution, the more accurate the interferometer if there is only one peak.

We also have looked at the case of an input state consisting of two number states with equal intensities (for which the amplitude fluctuations are zero). From our analysis, we have found that sensitivity of the interferometer depends not only on the width of the peaks but also on the number of peaks and their locations. For example, narrow peaks can provide poor sensitivity because their contributions cancel. For the number state inputs with equal intensities, there are two identical sharp peaks at $\theta_d = 0$ and $\theta_d = \pi$ with the width of each peak of order of $1/n$ where n is number of photons in one of the input ports. However, because of the locations of the peaks, their contributions to the sensitivity cancel each other totally; there is no signal to measure. If we have one narrow peak at either $\theta_d = 0$ or $\theta_d = \pi$, we could have taken the advantage of the sharp peak in the difference phase distribution. Or if we have two peaks located at $\theta_d = 0$ and $\theta_d = \pi$ with different height, then their contributions no longer cancel each other. We have found that for input state with a linear combination of number states. there are two peaks at zero and π and the peak at zero is higher than the peak at π. Therefore, their contributions do not cancel each other totally. Thus, for this input state, we could utilize the narrow width of the peaks and found the accuracy of the interferometer is in the order of $1/n$ where n is the number of photons in one of the input ports of the input beam.

Finally, we have examined the role of losses. As expected losses degraded sensitivity and we gave an estimate for the relation between these quantities. We

have determined relation between how great the losses are, and how much the accuracy is degraded. We also have found that for large photon numbers, the effect of losses on a state with a sharply peaked phase distribution is larger than on a state whose phase is less well defined.

References

[1] L. Susskind and J. Glowgower, Physics 1,49 (1964).

[2] P. Carruthers and M. Nieto. Rev. Mod. Phys. **40**. 411 (1968).

[3] Quantum Phase and Phase-Dependent Measurments, edited by W. P. Schleich and S. M. Barnett, special issue of Phys. Scr. **T48** (1993).

[4] S. Barnett and D. Pegg, J. Phys. Opt. **19**, 3849 (1986).

[5] S. Barnett and D. Pegg, J. Mod. Opt. **36**, 7 (1989).

[6] B. Yurke, S. McCall. and J. Klauder, Phys. Rev. A. **33**. 4033 (1986).

[7] M. Hillery and L. Mlodinow, Phys. Rev. A. **48**. 1548 (1993).

[8] M. Hillery, M. Freyberger. and W. Schleich Phys. Rev. A. **51**. 1792 (1995).

[9] M. Holland and K. Burnett, Phys. Rev. Lett. **71**, 1355 (1993).

[10] M. Hillery, M Zou, and V. Buzek, Quantum and Semiclass. Opt. **8**. 1041 (1996).

[11] A D. F. Walls and G. J. Milburn, Quantum Optics (Springer-Verlag. New York, 1994).

[12] J. H. Shapiro, S. R. Shepard, Phys. Rev. A **43**, 3795 (1990).

[13] R. J. Glauber, Phys. Rev. **B1**, 2766 (1963).

[14] M. Bonn and E. Wolf, Principles of Optics (Pergamon, Oxford, 1975).

[15] J. Schwinger, in Quantum Theory of Anguler Momentum, edited by C. Beidenharn and H. Van Dam (Academic, New York, 1965).

[16] R. A. Campos, B. E. A. Saleh, and M. C. Teich, Phys. Rev. **40**,1371 (1989).

[17] F. Singer, R. A. Campos, and B. E. A. Saleh, Quantum Optics. **2**. 307 (1990).

[18] D. F. Walls, Nature **324**. 210 (1986).

[19] C. M. Caves. Phys. Rev. D **23**. 1693 (1981).

[20] R. Loudon. The Quantum Theory of Light (Oxford Univ. Press. Oxford. 1973).

[21] B. Yurke (Unpublished paper).

[22] T. Kim, O. Pfister, M. J. Holland, J. Noh and J. Hall. Phys. Rev. A **57**. 4004 (1988).

[23] I. S. Gradshteyn and I. M. Ryzhik. Table of Integration. Series and Products (Academic Press, New York, 1994).

IMAGE EVALUATION TEST TARGET (QA-3)

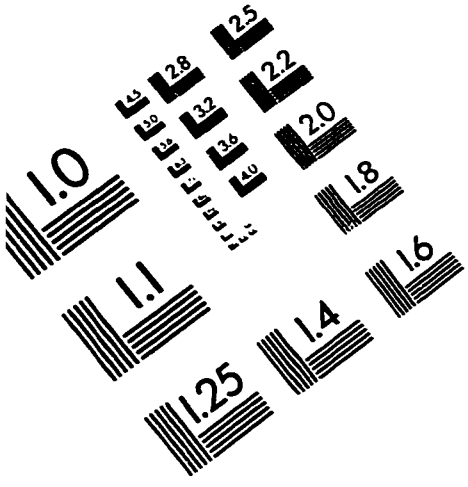

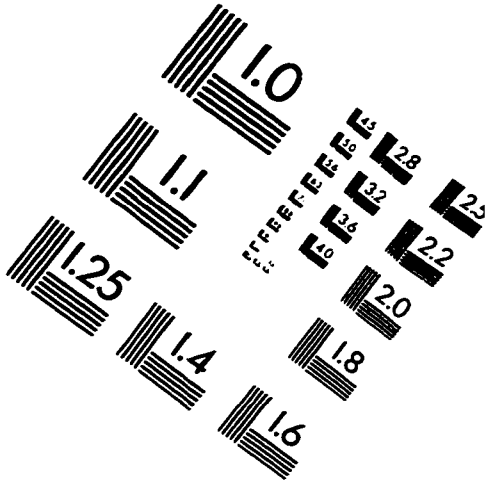

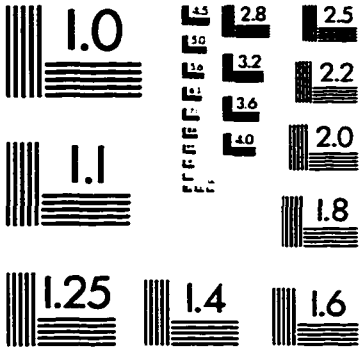

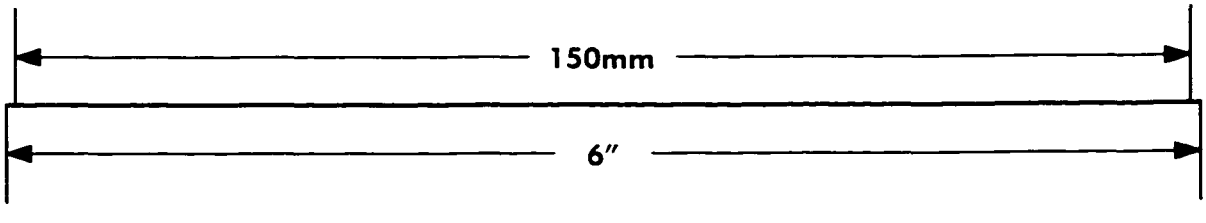

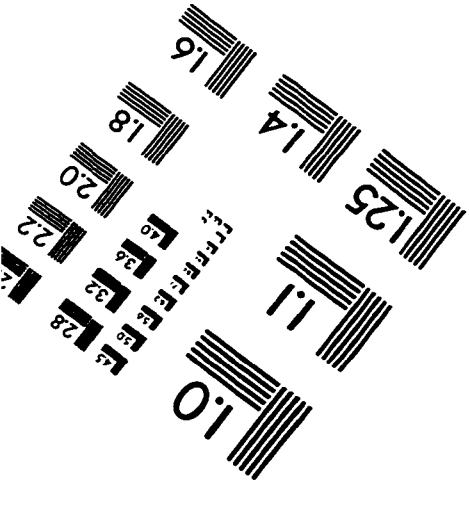

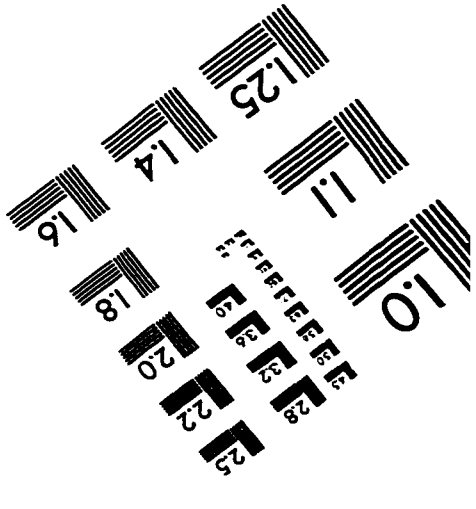

APPLIED IMAGE, Inc
1653 East Main Street
Rochester, NY 14609 USA
Phone: 716/482-0300
Fax: 716/288-5989